

# Intrinsic mechanisms for drive-dependent Purcell decay in superconducting quantum circuits

Ryo Hanai<sup>1,2</sup>, Alexander McDonald<sup>2,3</sup>, and Aashish Clerk<sup>2</sup>

<sup>1</sup>Asia Pacific Center for Theoretical Physics, Pohang 37673, Korea

<sup>2</sup>Pritzker School of Molecular Engineering, University of Chicago, Chicago, Illinois 60637, USA

<sup>3</sup>Department of Physics, University of Chicago, Chicago, Illinois 60637, USA



(Received 17 June 2021; accepted 9 December 2021; published 30 December 2021)

We develop an approach to understanding intrinsic mechanisms that cause the  $T_1$ -decay rate of a multilevel superconducting qubit to depend on the photonic population of a coupled, detuned cavity. Our method yields simple analytic expressions for both the coherently driven or thermally excited cases, which are in good agreement with full master equation numerics, and also facilitates direct physical intuition. It also predicts several interesting phenomena. In particular, we find that in a wide range of settings, the cavity-qubit detuning controls whether a nonzero photonic population increases or decreases qubit Purcell decay. Our method combines insights from a Keldysh treatment of the system, and Lindblad perturbation theory.

DOI: [10.1103/PhysRevResearch.3.043228](https://doi.org/10.1103/PhysRevResearch.3.043228)

## I. INTRODUCTION

Circuit quantum electrodynamics (cQED) systems based on superconducting circuits [1,2] are a leading platform for quantum information processing [3], and for explorations of basic quantum-optical and many-body phenomena [4,5]. The study of quantum dissipation in these systems is also of crucial interest (see, e.g., [6–12]). In many respects, the physics of cQED systems parallel that of atomic cavity QED systems. cQED systems incorporate nonlinear Josephson junction circuits that mimic artificial atoms, and linear microwave cavities that mimic photonic cavities. A paradigmatic dissipative effect in cavity QED is Purcell decay [13], the modification of atomic decay by a cavity. cQED systems motivate studying a modified version of this effect: What happens to Purcell decay when the cavity is now populated with photons (either by coherent driving or thermal noise)? This is of crucial relevance to understanding the experimentally-observed excess qubit decay during dispersive measurement [14,15] as well as the effect of background thermal radiation on qubit coherence.

Surprisingly, a full understanding of how a photonic population impacts Purcell decay (in a form relevant to cQED) is currently lacking. Reference [9] analyzed a driven Jaynes-Cummings (JC) model (i.e., a two-level qubit), finding that populating a cavity increases the qubit  $T_1$ -decay time (see also [6]). A similar trend was found in [16], which used a closely related Golden-Rule calculation to study a multilevel transmon qubit. However, in a more recent work in Refs. [11,12] that extended blackbox quantization theory [17] to describe transmon-cavity systems, an opposite-signed ef-

fect, i.e., decreasing  $T_1$  with increasing cavity photon number, was numerically suggested. Unfortunately, the complexity of the method did not lend itself to simple analytic expressions nor to an intuitive picture of the underlying physics.

In this paper, we introduce a theoretical approach to understanding Purcell decay in transmon-cavity systems in the presence of driving that complements and extends previous studies. Our approach combines insights from Keldysh theory with Lindblad perturbation theory (see, e.g., [18,19]). It provides compact *analytic* expressions that could be easily compared against experiment, and also facilitates simple intuitive explanations. It also reveals several surprising effects not previously discussed. In particular, we show that whether or not  $T_1$  increases or decreases with cavity drive is crucially dependent on the *sign* of the cavity-qubit frequency detuning (Figs. 1 and 2). We also analyze the impact of thermal cavity photons, and show that the basic physics in this case is strikingly different from the coherent-drive case. In the thermal case, the unexpected interplay between a nonresonant dissipative process and a nonresonant Hamiltonian process yields the dominant contribution. We discuss how this process would be completely missed if one resorted to standard secular approximations or considered a JC model instead of the transmon-cavity model analyzed here. Our paper reveals new understanding into the basic quantum dissipative mechanisms of driven circuit QED systems. It also outlines an analytic approach that could be useful in studying a host of driven-dissipative systems.

## II. TRANSMON MODEL AND THEORETICAL FRAMEWORK

We consider a standard setup where a multilevel transmon-style superconducting qubit is coupled to a linear microwave resonator, with each system subject to dissipation. We first consider the case with no coherent driving; this will be analyzed later. The total Hamiltonian is  $\hat{H} = \hat{H}_s + \hat{H}_{\text{diss}}$ , with  $\hat{H}_s$

Published by the American Physical Society under the terms of the [Creative Commons Attribution 4.0 International license](https://creativecommons.org/licenses/by/4.0/). Further distribution of this work must maintain attribution to the author(s) and the published article's title, journal citation, and DOI.

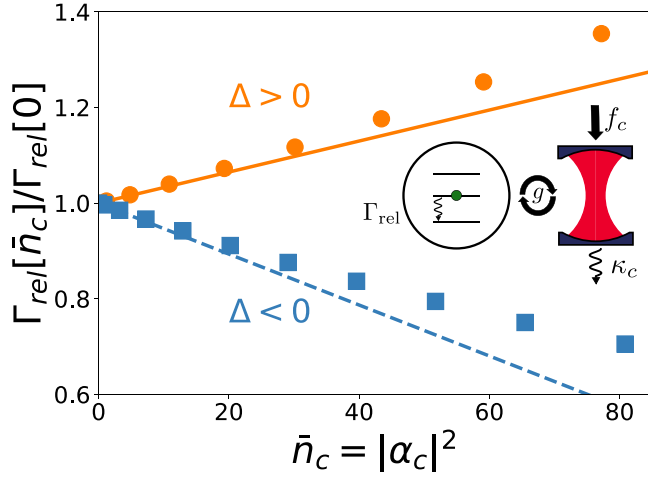


FIG. 1. Inset: Schematic of a cavity coupled to a weakly anharmonic qubit. Main: Qubit  $T_1$ -decay rate  $\Gamma_{\text{rel}}$  as a function of drive-induced cavity photon number  $\bar{n}_c = |\alpha_c|^2$ . Orange indicates results for a positive qubit-cavity detuning  $\Delta = \omega_a - \omega_c > 0$ , blue for a negative detuning. Solid symbols are master equation numerics, solid lines correspond to our analytic result [Eq. (20)]. One sees a striking dependence on the sign of  $\Delta$ . Parameters correspond to a qubit cavity coupling  $g = 0.1|\Delta|$ , qubit nonlinearity  $U = 0.1|\Delta|$ , cavity damping rate  $\kappa_c = 0.01|\Delta|$ , and drive frequency  $\omega_D = \omega_c - 0.1|\Delta|$ . Setting  $|\Delta|/(2\pi) = 1\text{GHz}$ , the above parameters correspond to  $U/(2\pi) = g/(2\pi) = 100\text{MHz}$  and  $\kappa_c/(2\pi) = 10\text{MHz}$ . All baths are at zero temperature, and we assume that qubit decay is only due to Purcell effects (i.e.,  $\kappa_a = 0$ ).

describing the isolated qubit and cavity, and  $\hat{H}_{\text{diss}}$  the dissipative environment and its coupling to the system. We will focus on regimes where the qubit can be treated as an anharmonic (Kerr) oscillator, hence

$$\hat{H}_s = \omega_a \hat{a}_0^\dagger \hat{a}_0 + g(\hat{a}_0^\dagger \hat{c}_0 + \text{H.c.}) + \omega_c \hat{c}_0^\dagger \hat{c}_0 - \frac{U}{2} \hat{a}_0^\dagger \hat{a}_0^\dagger \hat{a}_0 \hat{a}_0. \quad (1)$$

Here,  $\hat{a}_0$  and  $\hat{c}_0$  are bosonic annihilation operators describing (bare) qubit and cavity excitations, with  $\omega_a$  and  $\omega_c$  their res-

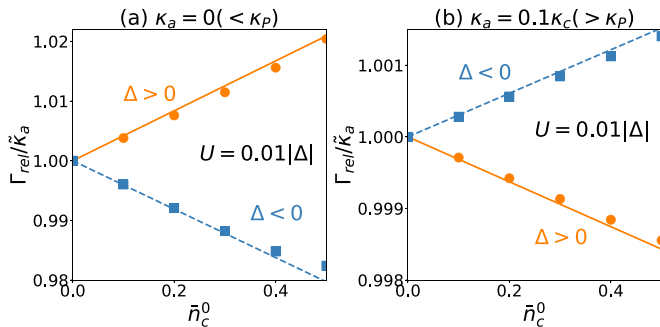


FIG. 2. Qubit  $T_1$ -decay rate  $\Gamma_{\text{rel}}$  as a function of cavity thermal population  $\bar{n}_c^0$ . The parameters are  $g = 0.1|\Delta|$ ,  $U = 0.01|\Delta|$ ,  $\kappa_c = 0.01|\Delta|$ ,  $\bar{n}_a = 0$ , with the bare qubit decay rate (a)  $\kappa_a = 0 (< \kappa_p \equiv (g^2/\Delta^2)(\kappa_c - \kappa_a))$  and (b)  $\kappa_a = 0.1\kappa_c (> \kappa_p)$ . The lines and points are our analytical [Eq. (14)] and numerical results, respectively. One sees that the sign of the temperature dependence depends both on detuning  $\Delta$  and on the ratio of the intrinsic qubit decay rate and the Purcell decay rate  $\kappa_a/\kappa_p$ .

onant frequencies. The qubit-cavity coupling is denoted by  $g$ , while  $U > 0$  is the Kerr nonlinearity of the qubit (obtained by expanding the full Josephson junction cosine potential [20]). We will be interested throughout in the typical regime where the cavity-qubit detuning  $\Delta = \omega_a - \omega_c$  may be comparable in magnitude to  $U$ , but where  $U \ll \omega_a, \omega_c$ . We also focus on modest drives and temperatures; together, this implies that additional nonlinear terms play no significant role [21].

We will further focus on the standard dispersive regime of cQED, where  $|g/\Delta|$  is small, but not so small that leading  $(g/\Delta)^2$  corrections can be ignored. We will work in the so-called “blackbox” basis [17], and thus first diagonalize the quadratic part of  $\hat{H}_s$ :  $\hat{H}_0 = \omega_c \hat{c}_0^\dagger \hat{c}_0 + g(\hat{a}_0^\dagger \hat{c}_0 + \text{H.c.}) + \omega_a \hat{a}_0^\dagger \hat{a}_0 = \tilde{\omega}_c \hat{c}^\dagger \hat{c} + \tilde{\omega}_a \hat{a}^\dagger \hat{a}$ . Here, dressed cavity and qubit “polariton” operators are given by  $\hat{c} \simeq [1 - g^2/(2\Delta^2)]\hat{c}_0 - (g/\Delta)\hat{a}_0$  and  $\hat{a} \simeq [1 - g^2/(2\Delta^2)]\hat{a}_0 + (g/\Delta)\hat{c}_0$ , respectively. The corresponding renormalized frequencies are  $\tilde{\omega}_a \simeq \omega_a + g^2/\Delta$  and  $\tilde{\omega}_c \simeq \omega_c - g^2/\Delta$ . The Kerr nonlinearity takes the form  $\hat{H}_{\text{int}} = -(U/2)\hat{a}_0^\dagger \hat{a}_0^\dagger \hat{a}_0 \hat{a}_0 \simeq \hat{H}_{\text{int}}^{\text{slf}} + \hat{H}_{\text{int}}^{\text{crs}} + \hat{H}_{\text{int}}^{\text{nc}} + \hat{V}_{\text{int}}$ . Here, the first two terms are usual self and cross-Kerr nonlinearities

$$\hat{H}_{\text{int}}^{\text{slf}} = \chi_{aa} \hat{a}^\dagger \hat{a}^\dagger \hat{a} \hat{a}, \quad \hat{H}_{\text{int}}^{\text{crs}} = \chi_{ca} \hat{c}^\dagger \hat{c} \hat{a}^\dagger \hat{a} \quad (2)$$

with  $\chi_{aa} = -(U/2)[1 - g^2/(2\Delta^2)]$  and  $\chi_{ca} = -2g^2U/\Delta^2$ . In contrast

$$\hat{H}_{\text{int}}^{\text{nc}} = \tilde{\chi}(\hat{a}^\dagger \hat{a}^\dagger \hat{a} \hat{c} + \hat{c}^\dagger \hat{a}^\dagger \hat{a} \hat{a}) \quad (3)$$

(with  $\tilde{\chi} = gU/\Delta$ ) describes a nonlinear process in which a cavity photon is converted into a qubit excitation (or vice versa) with an amplitude that depends on qubit excitation number. While this process is nonresonant, it will play a crucial role in mediating photon-number dependent dissipative effects. Finally, the last interaction term  $\hat{V}_{\text{int}}$  contains nonresonant terms of order  $(g/\Delta)^3$  or higher, and will play no role in what follows; we thus set it to zero. We will often refer to the cavity/qubit polariton modes  $\hat{c}$  and  $\hat{a}$  as simply the “cavity/qubit modes”, while  $\hat{c}_0$  and  $\hat{a}_0$  will be called the “bare modes”.

We now turn to the modeling of dissipation. As is standard, we take the bare qubit and cavity to each be coupled linearly to independent, Markovian bosonic reservoirs [1,2] (though certain extensions to non-Markovian cavity baths are discussed below). Using a Keldysh approach, one can integrate out these reservoirs and derive a formally exact dissipative action describing the system. As shown in the Appendix A, in the small dissipation limit of interest, this action is equivalent to the following Lindblad master equation:

$$\partial_t \hat{\rho} = -i[\hat{H}_s, \hat{\rho}] + \sum_{\mu=a,c} \kappa_\mu [(1 + \bar{n}_\mu^0) \mathcal{D}[\hat{d}_\mu^0] \hat{\rho} + \bar{n}_\mu^0 \mathcal{D}[\hat{d}_\mu^{0\dagger}] \hat{\rho}] \equiv \mathcal{L} \hat{\rho}, \quad (4)$$

where  $\hat{d}_c^0 = \hat{c}_0$ ,  $\hat{d}_a^0 = \hat{a}_0$ , and  $\kappa_\mu (\bar{n}_\mu^0)$  are the decay rates (thermal occupancies) of the bare cavity and qubit environments. We also take  $\mathcal{D}[\hat{L}] \rho = \hat{L} \rho \hat{L}^\dagger - \frac{1}{2} \{\hat{L}^\dagger \hat{L}, \rho\}$  as the usual Lindblad dissipator. In what follows, we will focus attention on the experimentally relevant regime where the cavity damping rate is much larger than the intrinsic qubit decay rate,  $\kappa_a \ll \kappa_c$ . As our focus is on describing Purcell decay, we do not include an intrinsic qubit dephasing dissipator [22].

Note that Eq. (4) describes a *dissipative* coupling between polariton modes. To see this explicitly, we transform it to the blackbox basis, where it takes the form

$$\partial_t \hat{\rho} = \mathcal{L} \hat{\rho} = \mathcal{L}_{\text{ind}} \hat{\rho} + \mathcal{L}_{\text{cd}} \hat{\rho}. \quad (5)$$

The Liouvillian  $\mathcal{L}_{\text{ind}}$  describes a model where each polariton is coupled to independent effective reservoirs; letting  $\hat{d}_c = \hat{c}$  and  $\hat{d}_a = \hat{a}$ , we have

$$\begin{aligned} \mathcal{L}_{\text{ind}} \hat{\rho} = & -i[\hat{H}_s, \hat{\rho}] \\ & + \sum_{\mu=a,c} \tilde{\kappa}_\mu [(1 + \tilde{n}_\mu) \mathcal{D}[\hat{d}_\mu] \hat{\rho} + \tilde{n}_\mu \mathcal{D}[\hat{d}_\mu^\dagger] \hat{\rho}]. \end{aligned} \quad (6)$$

The damping rates and thermal occupancies corresponding to the effective qubit-polariton bath are given by

$$\tilde{\kappa}_a = \kappa_a + \frac{g^2}{\Delta^2} (\kappa_c - \kappa_a) \equiv \kappa_a + \kappa_P, \quad (7)$$

$$\tilde{n}_a = \frac{1}{\tilde{\kappa}_a} \left[ \kappa_a \bar{n}_a^0 + \frac{g^2}{\Delta^2} (\kappa_c \bar{n}_c^0 - \kappa_a \bar{n}_a^0) \right]. \quad (8)$$

The cavity-polariton bath parameters  $\tilde{\kappa}_c$  and  $\tilde{n}_c$  are given by analogous expressions (one simply exchanges  $c$  and  $a$ ). Note that the qubit-polariton decay rate in Eq. (7) is simply the sum of the intrinsic qubit decay rate  $\kappa_a$  and standard (zero temperature) Purcell decay rate  $\kappa_P$ .

Equation (6) also has a term  $\mathcal{L}_{\text{cd}}$  describing *correlated dissipation* that provides a dissipative coupling of qubit and cavity polaritons:

$$\begin{aligned} \mathcal{L}_{\text{cd}} \hat{\rho} = & -\frac{1}{2} (\tilde{\gamma}_\uparrow + \tilde{\gamma}_\downarrow) \{ \hat{a}^\dagger \hat{c} + \hat{c}^\dagger \hat{a}, \hat{\rho} \} \\ & + \tilde{\gamma}_\downarrow (\hat{a} \hat{\rho} \hat{c}^\dagger + \hat{c} \hat{\rho} \hat{a}^\dagger) + \tilde{\gamma}_\uparrow (\hat{a}^\dagger \hat{\rho} \hat{c} + \hat{c}^\dagger \hat{\rho} \hat{a}), \end{aligned} \quad (9)$$

where

$$\tilde{\gamma}_\downarrow = (g/\Delta) [\kappa_c (1 + \bar{n}_c^0) - \kappa_a (1 + \bar{n}_a^0)] \quad (10)$$

$$\tilde{\gamma}_\uparrow = (g/\Delta) [\kappa_c \bar{n}_c^0 - \kappa_a \bar{n}_a^0]. \quad (11)$$

The first line in Eq. (9) describes an effective non-Hermitian beam-splitter coupling between polaritons, whereas the last line describes correlated noise.

We stress again that the correlated polariton dissipation described by Eq. (9) follows from our exact treatment. Nonetheless, it is common at this point to simply omit  $\mathcal{L}_{\text{cd}}$ . This corresponds to a standard secular approximation: as  $\mathcal{L}_{\text{cd}}$  describes nonresonant processes (detuning  $\sim \Delta$ ), and as  $|\Delta| \gg \tilde{\gamma}_\uparrow, \tilde{\gamma}_\downarrow$ ,  $\mathcal{L}_{\text{cd}}$  is expected to have a marginal effect. We will not make this approximation in what follows [23]. Surprisingly, we show that in the case of a thermal cavity population, the correlated dissipation described by  $\mathcal{L}_{\text{cd}}$  provides the dominant temperature-dependent correction to the qubit Purcell decay rate.

### III. QUBIT DECAY RATE IN THE PRESENCE OF TEMPERATURE

We can now examine how qubit dissipation is modified by populating the cavity. The general picture is that nonresonant coupling processes (both Hamiltonian and dissipative) will alter the Purcell contribution to the qubit  $T_1$  population decay

rate  $\Gamma_{\text{rel}}$ . Our approach will be to treat these processes systematically using Lindblad perturbation theory (see Appendix B for a short review). To this end, we write our full Liouvillian as  $\mathcal{L} = \mathcal{L}_0 + \mathcal{L}_1$ , where  $\mathcal{L}_0$  describes *all processes which do not couple qubit and cavity polaritons*. In contrast,  $\mathcal{L}_1$  describes both nonlinear and dissipative polariton-polariton coupling terms:

$$\mathcal{L}_1 \hat{\rho} = -i[\epsilon_{\text{crs}} \hat{H}_{\text{int}}^{\text{crs}} + \epsilon_{\text{ns}} \hat{H}_{\text{int}}^{\text{nc}}, \hat{\rho}] + \epsilon_{\text{nc}} \mathcal{L}_{\text{cd}} \hat{\rho}, \quad (12)$$

$\mathcal{L}_1$  will be treated perturbatively, as it scales as the small parameter  $g/\Delta$ . To make the physical origin of different contributions clear in what follows, we have introduced book-keeping constants  $\epsilon_{\text{crs}} = \epsilon_{\text{ns}} = \epsilon_{\text{cd}} = 1$ . We stress that the qubit self-Kerr interaction  $\hat{H}_{\text{int}}^{\text{slf}}$  in Eq. (2) is included in  $\mathcal{L}_0$ .

The first step is to identify the qubit  $T_1$ -decay mode to zeroth order in perturbation theory. This can be done unambiguously, as  $\mathcal{L}_0$  has a set of eigenmodes, which *only* describe qubit population decay (in the Fock basis). We identify the eigenvalue of the *slowest* of these eigenmodes as the qubit  $T_1$ -decay rate  $\Gamma_{\text{rel}}$ ; it dominates the relaxation of an initial qubit excited state. We find [24–26] (see Appendix C)

$$\Gamma_{\text{rel}}^{(0)} = \tilde{\kappa}_a = \kappa_a + \frac{g^2}{\Delta^2} (\kappa_c - \kappa_a). \quad (13)$$

Note that this leading-order decay rate is independent of both the temperature  $\bar{n}_\mu^0$  and the self-Kerr nonlinearity  $\chi_{aa}$ , as has been noted in other contexts (see, e.g., [27]).

We next calculate the leading-order correction to  $\Gamma_{\text{rel}}$  arising from  $\mathcal{L}_1$ . This amounts to perturbatively calculating the eigenvalue shift of the relevant Liouvillian eigenmode, which emerges at second order. Focusing on the experimentally relevant regime of weak intrinsic qubit loss ( $|\chi_{aa}| \sim U \gg \tilde{\kappa}_a$ ) and low temperature ( $\bar{n}_c^0, \bar{n}_a^0 \ll 1$ ), a straightforward but tedious calculation yields (see Appendix C for derivation),

$$\begin{aligned} \Gamma_{\text{rel}} \simeq & \tilde{\kappa}_a + \frac{g^2}{\Delta^2} \frac{\epsilon_{\text{cd}} \epsilon_{\text{nc}} U}{\Delta - U} [8(\kappa_c - \kappa_a) \tilde{n}_a - 4(\kappa_c \bar{n}_c^0 - \kappa_a \bar{n}_a^0)] \\ & + \frac{g^2}{\Delta^2} \frac{\epsilon_{\text{nc}}^2 U^2}{(\Delta - U)^2} (\tilde{\kappa}_a + \tilde{\kappa}_c) (4\tilde{n}_a - 2\tilde{n}_c), \end{aligned} \quad (14)$$

where all neglected terms are  $\mathcal{O}[(g/\Delta)^4]$  or higher. This is the first main result of this paper. The second and third terms here describe temperature-dependent contributions to Purcell decay. We find a surprising dependence both on bath temperatures, and on *the sign* of the qubit cavity detuning  $\Delta$ . The third term in Eq. (14)  $\propto \epsilon_{\text{nc}}^2$  is solely due to the nonlinear conversion process in Eq. (3), and can be linked to Fermi's Golden rule rates involving the qubit  $n = 2$  state (see Appendix C). More interesting is the second term ( $\propto \epsilon_{\text{cd}} \epsilon_{\text{nc}}$ ), which dominates the third term in the usual limit where  $\Delta \gtrsim U$ . This process results from a subtle interplay between the Hamiltonian nonlinear conversion interaction, and the dissipative polariton coupling described by  $\mathcal{L}_{\text{cd}}$ . Note that both correction terms vanish at zero temperature.

The surprising interplay of coherent and dissipative conversion processes in determining qubit relaxation can be understood intuitively. Consider a model of two linear classical oscillators whose amplitudes  $\beta_a, \beta_c$  obey:

$$i\partial_t \begin{pmatrix} \beta_c \\ \beta_a \end{pmatrix} = \begin{pmatrix} \tilde{\omega}_c - i\tilde{\kappa}_c/2 & r - i\gamma \\ r - i\gamma & \tilde{\omega}_a - i\tilde{\kappa}_a/2 \end{pmatrix} \begin{pmatrix} \beta_c \\ \beta_a \end{pmatrix}. \quad (15)$$

This describes two modes with resonant frequencies  $\tilde{\omega}_c, \tilde{\omega}_a$ , decay rates  $\tilde{\kappa}_c, \tilde{\kappa}_a$  that are coupled both coherently (rate  $r$ ) and dissipatively (rate  $\gamma$ ), which roughly mimics the nonlinear conversion and correlated dissipation, respectively. For weak couplings, the eigenmodes of the above dynamical matrix remain localized. A simple diagonalization shows that the decay rate for the  $a$ -like mode is modified by the couplings as  $\tilde{\kappa}_a \rightarrow \tilde{\kappa}_a + 2\gamma r / (\tilde{\omega}_a - \tilde{\omega}_c) + \mathcal{O}(r^2)$ . We see that the dominant shift in the lifetime involves the *product* of dissipative and coherent couplings, in direct analogy to Eq. (14). Of course, in our system nonlinearity modifies the form of the correction. Still, the basic mechanism involving coherent and dissipative couplings working in consort is the same (as is the striking dependence on the sign of the detuning, reflecting an avoided crossing).

Another striking prediction of Eq. (14) is that the sign of the dominant temperature-dependent term is sensitive to the relative importance of Purcell decay to intrinsic qubit decay. For  $\kappa_P \gg \kappa_a$ , Eq. (8) tells us that  $\tilde{n}_a \approx \tilde{n}_c \approx \tilde{n}_c^0$ , whereas for  $\kappa_P \ll \kappa_a$  we have  $\tilde{n}_a \ll \tilde{n}_c^0$ . It follows that in these two limiting cases, Eq. (14) can be approximated as

$$\Gamma_{\text{rel}} \simeq \tilde{\kappa}_a \pm \frac{4g^2}{\Delta^2} \frac{U}{\Delta - U} \kappa_c \tilde{n}_c^0, \quad (16)$$

where  $+$  ( $-$ ) corresponds to  $\kappa_P \gg \kappa_a$  ( $\kappa_P \ll \kappa_a$ ). We see that the impact of a cavity thermal population is opposite in these two regimes.

The results of Eq. (14) are numerically confirmed in Fig. 2, where we compare against a direct master equation simulation of Eq. (5) [28,29] using experimentally-relevant parameters [3]. The numerical  $T_1$ -decay rate corresponds to the time-dependent decay of an initial state where an excitation is added to the qubit (see Appendix E for details). Our analytic, perturbative expressions quantitatively agree the numerical results at low temperatures and small-to-modest nonlinearity. The qualitative agreement at larger nonlinearity  $U = 0.1|\Delta|$  is also reasonable (see Fig. 3), though here, higher order contributions become important, especially if  $\kappa_a < \kappa_P$ . (See Appendix C for a detailed discussion on this point.)

#### IV. QUBIT DECAY RATE IN THE PRESENCE OF COHERENT DRIVE

Consider now a coherent linear driving of the cavity, as described by the additional system Hamiltonian term  $\hat{H}_D = f_c e^{-i\omega_D t} \hat{c}_0 + \text{H.c.}$  We move to a rotating frame at the drive frequency  $\omega_D$ , which effectively shifts  $\omega_\mu \rightarrow \omega_\mu - \omega_D$ . We further make a standard displacement transformation of both modes:  $\mathcal{L}' = \hat{D}^\dagger[\alpha_c, \alpha_a] \mathcal{L} \hat{D}[\alpha_c, \alpha_a]$ , where  $\hat{D}[\alpha_c, \alpha_a]$  is a displacement operator that displaces the bare cavity (qubit) operator  $\hat{c}_0(\hat{a}_0)$  by the time-independent amplitude  $\alpha_c(\alpha_a)$ . By choosing displacements to cancel linear terms, the displaced Lindbladian  $\mathcal{L}'$  has the same dissipative terms as  $\mathcal{L}$  in Eq. (4), but a modified system Hamiltonian  $\hat{H}'_s = \hat{H}_0 + \hat{H}'_{\text{int}} = \hat{H}_0 + \hat{D}^\dagger[\alpha_c, \alpha_a] \hat{H}_{\text{int}} \hat{D}[\alpha_c, \alpha_a]$ . For weak drives with small induced amplitudes  $|\alpha_a|^2 \ll 1$ , it is sufficient to only keep terms in  $\hat{H}'_{\text{int}}$  that are at most  $\mathcal{O}[\alpha_a^2]$ :

$$\hat{H}'_{\text{int}} \simeq \hat{H}_{\text{int}} - U(\alpha_a \hat{a}_0^\dagger \hat{a}_0^\dagger + \text{H.c.}) + \hat{H}_{\text{quad}} \quad (17)$$

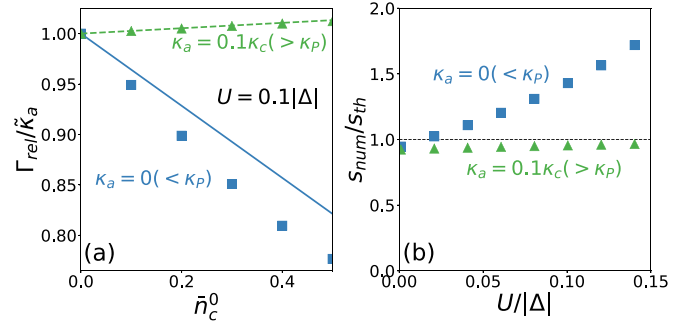


FIG. 3. (a) Thermal cavity drive dependence on the qubit  $T_1$ -decay rate  $\Gamma_{\text{rel}}$  for a larger nonlinearity  $U = 0.1|\Delta|$ . Lines (points) correspond to analytical (numerical) results. Higher-order corrections are more important here, but the analytic results still give good qualitative agreement. (b) The ratio of the numerically ( $s_{\text{num}}$ ) to analytically ( $s_{\text{th}}$ ) evaluated slope parameter  $s = d\Gamma_{\text{rel}}/d\tilde{n}_c^0$  (evaluated at zero temperature). For both the panels, we set  $g = 0.1|\Delta|$ ,  $\kappa_c = 0.01|\Delta|$  and  $\Delta < 0$ . For large  $U$  and  $\kappa_P > \kappa_a$ , higher-order corrections become important (as discussed in Appendix C), but our analytical expression still provides a reasonable qualitative agreement.

The second term here describes an effective nonlinear single photon drive, whereas

$$\hat{H}_{\text{quad}} = -2U|\alpha_a|^2 \hat{a}_0^\dagger \hat{a}_0 - \frac{U}{2}(\alpha_a^2 \hat{a}_0^\dagger \hat{a}_0^\dagger + \text{H.c.}) \quad (18)$$

describes a mean-field frequency shift and weak squeezing drive. As these terms are quadratic, they can be accounted for exactly by defining our blackbox polaritons to be the eigenmodes of  $\hat{H}_0 + \hat{H}_{\text{quad}}$ . The squeezing terms will play no role in what follows, so we drop them. The remaining frequency shift terms then lead to a modification of the qubit-cavity detuning  $\Delta$ :  $\Delta \rightarrow \Delta - 2U|\alpha_a|^2 \equiv \Delta'[\alpha_a]$ .

The modification of the qubit polariton by the drive directly leads to a modification of  $\tilde{\kappa}_a$ , the intrinsic (linear-theory) qubit polariton damping rate:

$$\begin{aligned} \tilde{\kappa}'_a[\alpha_a] &= \kappa_a + \frac{g^2}{(\Delta'[\alpha_a])^2} (\kappa_c - \kappa_a) \\ &\simeq \kappa_a + \kappa_P + \frac{g^2}{\Delta^2} \frac{4U}{\Delta} (\kappa_c - \kappa_a) |\alpha_a|^2, \end{aligned} \quad (19)$$

where in the last line we have expanded to leading order in  $|\alpha_a|^2$ . We see that the simple mean-field shift of the cavity frequency directly yields a change in the linear-theory polariton decay rate, one that is odd in  $\Delta$ . This term simply reflects the modified qubit-cavity hybridization resulting from the drive-induced cavity frequency shift. The fact that driving a nonlinear system gives rise to a notion of drive dependent polaritons has been discussed in many different contexts (see, e.g., [30]).

To calculate the full modification of the qubit  $T_1$  decay, we must also include the perturbative contribution of the  $\mathcal{O}[\alpha_a]$  nonlinear drive term in Eq. (17). Again using Lindblad perturbation theory, as derived in Appendix D, we finally obtain (for

zero temperature, and to order  $\mathcal{O}[|\alpha_a|^2]$ :

$$\Gamma_{\text{rel}} \simeq \tilde{\kappa}'_a[\alpha_a] - \frac{2U^2}{(\tilde{\omega}_a - \omega_D - U)^2} \tilde{\kappa}_a |\alpha_a|^2. \quad (20)$$

This is the second main result of this paper. Note this result is contingent on a perturbative treatment of Eq. (17) being valid, which requires drive detuning  $|\tilde{\omega}_a - \omega_D - U| \gg \tilde{\kappa}_a$ . For the typical experimental scenario where the bare cavity decay rate dominates that of the qubit (i.e.,  $\kappa_a \ll \kappa_c$ ), the drive-dependence of the qubit  $T_1$ -decay rate is dominated by that of  $\tilde{\kappa}'_a[\alpha_a]$ . The sign of the drive dependence thus exhibits a striking dependence on the sign of  $\Delta$ . Our results are in excellent agreement with full master equation numerics, see Fig. 1. The fact that driving the cavity can either increase or decrease qubit  $T_1$  depending on  $\Delta$  was not noted in previous work. Note that this result is easily extended to the case where the intrinsic cavity bath has a different density of states at  $\omega = \omega_c$  and  $\omega = \omega_a$ , see Eq. (A34) in Appendix A.

## V. COMPARISON TO JAYNES-CUMMINGS MODEL

In this section, we compare our main results for the transmon model against the more commonly used JC model. As we have shown in the previous sections, in the transmon model, the presence of the qubit  $n = 2$  Fock state played a crucial role in determining the dissipative properties [see the discussions below Eq. (14)]. Therefore, we expect the JC model, which treats the qubit as a two-level system, to give very different results from our transmon model results. Here, we show that the dissipative properties of the JC model is indeed very different from the transmon model for both the thermal and coherent drive cases.

The equation of motion of the JC model is given by

$$\partial_t \hat{\rho} = -i[\hat{H}_{\text{JC}}, \hat{\rho}] + \kappa_c [(1 + \tilde{n}_c^0) \mathcal{D}[\hat{c}_0] \hat{\rho} + \tilde{n}_c^0 \mathcal{D}[\hat{c}_0^\dagger] \hat{\rho}] \quad (21)$$

where  $\hat{H}_{\text{JC}} = \hat{H}_0^{\text{JC}} + \hat{V}_{\text{JC}} + \hat{H}_D$  with

$$\hat{H}_0^{\text{JC}} = \omega_a \hat{\sigma}_z + \omega_c \hat{c}_0^\dagger \hat{c}_0, \quad (22)$$

$$\hat{V}_{\text{JC}} = g(\hat{\sigma}_+ \hat{c}_0 + \hat{\sigma}_- \hat{c}_0^\dagger). \quad (23)$$

Here,  $\hat{\sigma}_z$  and  $\hat{\sigma}_\pm = (\hat{\sigma}_x \pm i\hat{\sigma}_y)/2$  are Pauli matrices and have assumed a vanishing bare qubit dissipation rate  $\kappa_a = 0$ .

We first consider the case where the thermal bare cavity occupancy is present but has no coherent drive. Treating the Rabi coupling term  $\mathcal{L}_1 \bullet = -i[\hat{V}_{\text{JC}}, \bullet]$  as the perturbation within the Lindblad perturbation theory, the qubit  $T_1$ -decay rate at low temperature  $\tilde{n}_c^0 \ll 1$  in the dispersive limit  $g/|\Delta| \ll 1$  can be computed within the second-order perturbation as,

$$\Gamma_{\text{rel}}^{\text{JC}} \approx \frac{g^2}{\Delta^2} \kappa_c (1 + 2\tilde{n}_c^0). \quad (24)$$

In stark contrast to the rich behavior seen in our Figs. 2 and 3(a), we find that the JC model *always* gives an increase of the qubit  $T_1$ -decay rate. This result can be understood by regarding the dissipative cavity as a bath for the qubit that has a Lorentzian spectrum  $S_c(\omega) = (\kappa_c/(2\pi))/[(\omega - \omega_c)^2 + \kappa_c^2/4]$ . The second-order process of the qubit-cavity coupling  $g$  gives rise to an effective dissipation rate to the qubit given by  $\gamma = 2\pi g^2 S_c(\omega = \omega_a) \approx g^2 \kappa_c / \Delta^2$  [31]. Since the cavity at

a finite temperature gives both the absorption and emission, the qubit  $T_1$ -decay rate can be estimated as  $\Gamma_{\text{rel}}^{\text{JC}} \approx \gamma(1 + 2\tilde{n}_c^0)$ , which coincides with Eq. (24).

Although our scheme can be applied to the coherently driven JC model, we do not provide it here since the coherent drive case is analyzed in detail in Ref. [9]. It is found that the drive *always* decreases the qubit  $T_1$ -decay rate. This is, again, in stark contrast to our result [Eqs. (19) and (20)] for the weakly-nonlinear oscillator that can give positive or negative contribution dependent on the sign of the detuning  $\Delta$ . This is not surprising, as the mean-field shift to the frequency, which was responsible for the sign change in the transmon model, is absent in the JC model.

## VI. CONCLUSION

We have presented a systematic formalism for analyzing dissipation in driven cQED systems, deriving simple expressions that describe the modification of qubit Purcell decay due to thermal or coherent photons. Our results highlight the importance of the sign of the cavity-qubit detuning, and the interplay between nonresonant coherent and dissipative processes.

We note that, in most experiments, it is likely that there are other extrinsic effects (e.g., drive-induced heating) that can also affect the photon-number dependence of qubit  $T_1$ -decay rate, causing them to vary experiment to experiment. Our contribution here is to set the “fundamental limit” to such photon-number dependent dissipation; the discovered *intrinsic* mechanisms are unavoidable, even if the extrinsic dissipation channels are terminated. More generally, our paper provides a set of tools that can also be applied to other relevant problems, e.g., dissipation in multicavity systems with transmon-mediated interactions as outlined in Appendix F.

## ACKNOWLEDGMENTS

This work was supported by the Department of Energy BES Quantum Information Science Program under Award No. DE-SC0020152.

## APPENDIX A: KELDYSH FORMALISM FOR MULTI-LEVEL SUPERCONDUCTING QUBIT

### 1. Derivation of master equation (4) via the Keldysh formalism

We derive here the master equation Eq. (4) by using the Keldysh formalism [32], which treats the effects of the dissipative baths exactly. Our starting point is a Hamiltonian  $\hat{H}$ , which describes the qubit and cavity coupled to two independent Markovian baths. By integrating out these baths, we obtain a Keldysh action that is identical to the one corresponding to the master equation Eq. (4) and thus the two theories are equivalent.

As in the main text, the Hamiltonian, which describes the qubit, cavity, and their environments takes the form

$$\hat{H} = \hat{H}_s + \hat{H}_{\text{diss}}. \quad (A1)$$

Here,  $\hat{H}_s$  is the system Hamiltonian [Eq. (1) in the main text] and

$$\hat{H}_{\text{diss}} = \hat{H}_{a,A} + \hat{H}_{c,C} + \hat{H}_A + \hat{H}_C \quad (A2)$$

describes the environment and its coupling to the system, with  $A$  and  $C$  labeling the independent baths coupled to the qubit and cavity respectively. The coupling between the environments and the system of interest take the standard form

$$\hat{H}_{a,A} = -i\sqrt{\kappa_a}(\hat{a}^\dagger \hat{\xi}_A - \hat{a} \hat{\xi}_A^\dagger), \quad (\text{A3})$$

$$\hat{H}_{c,C} = -i\sqrt{\kappa_c}(\hat{c}^\dagger \hat{\xi}_C - \hat{c} \hat{\xi}_C^\dagger). \quad (\text{A4})$$

We assume that the baths are a collection of independent harmonic oscillators in a Gaussian state, which is captured by the terms  $\hat{H}_A$  and  $\hat{H}_C$ . The operators  $\hat{\xi}_A$  and  $\hat{\xi}_C$  are linear combination of bath annihilation operators.

Due to the Gaussian nature of the baths and the linear coupling, all the information on how they affect the system is captured by the relevant two-point correlation functions (which can be frequency-dependent). As with any theory where the path integral plays the central role, we must first identify the action. The Keldysh action corresponding to the Hamiltonian of Eq. (A1) can be written as [32]

$$S = S_s + S_{a,A} + S_{c,C} + S_A + S_C. \quad (\text{A5})$$

The first term describes the coherent dynamics between the qubit and the cavity, while the last two terms  $S_A$  and  $S_C$  describe the dynamics of a set of independent harmonic oscillators. The terms  $S_{a,A}$  and  $S_{c,C}$  describe the system-environment coupling. By defining the complex vectors

$$\mathbf{a}^\dagger(t) = (a_{\text{cl}}^*(t) \ a_{\text{q}}^*(t)), \quad \mathbf{c}^\dagger(t) = (c_{\text{cl}}^*(t) \ c_{\text{q}}^*(t)), \quad (\text{A6})$$

$$\hat{\xi}_A^\dagger(t) = (\xi_{A,\text{cl}}^*(t) \ \xi_{A,\text{q}}^*(t)), \quad \hat{\xi}_C^\dagger(t) = (\xi_{C,\text{cl}}^*(t) \ \xi_{C,\text{q}}^*(t)), \quad (\text{A7})$$

where cl and q label the classical and quantum fields, respectively, we can write the system-environment coupling terms in the action as

$$S_{a,A} = i\sqrt{\kappa_a} \int_{-\infty}^{\infty} dt (\mathbf{a}^\dagger(t) \sigma_x \hat{\xi}_A(t) - \hat{\xi}_A^\dagger(t) \sigma_x \mathbf{a}(t)) \quad (\text{A8})$$

$$S_{c,C} = i\sqrt{\kappa_c} \int_{-\infty}^{\infty} dt (\mathbf{c}^\dagger(t) \sigma_x \hat{\xi}_C(t) - \hat{\xi}_C^\dagger(t) \sigma_x \mathbf{c}(t)) \quad (\text{A9})$$

where  $\sigma_x$  is a Pauli matrix. Similarly, the system term  $S_s$  can be written as a function of complex vectors  $\mathbf{a}(t)$  and  $\mathbf{c}(t)$ , with its form reflecting the system Hamiltonian  $\hat{H}_s$ . The environment terms  $S_A, S_C$  are quadratic functions of  $\hat{\xi}_A$  and  $\hat{\xi}_C$ .

We now want a description of our system, which only involves the qubit and cavity modes. When working directly with the density matrix, this means tracing over the bath degrees of freedom. In the context of the path integral, the analogous step is to integrate over all bath fields. To do so, we first make a linear transformation to each bath field

$$\hat{\xi}_A(t) \rightarrow \hat{\xi}_A(t) + i\sqrt{\kappa_a} \int_{-\infty}^{\infty} dt' \mathbf{G}_A(t-t') \sigma_x \mathbf{a}(t') \quad (\text{A10})$$

$$\hat{\xi}_C(t) \rightarrow \hat{\xi}_C(t) + i\sqrt{\kappa_c} \int_{-\infty}^{\infty} dt' \mathbf{G}_C(t-t') \sigma_x \mathbf{c}(t') \quad (\text{A11})$$

where  $\mathbf{G}_A(t)$  and  $\mathbf{G}_C(t)$  are the matrix Green's function of the baths

$$\mathbf{G}_A(t) = \begin{pmatrix} -i\langle\{\hat{\xi}_A(t), \hat{\xi}_A^\dagger(0)\}\rangle & -i\Theta(t)\langle[\hat{\xi}_A(t), \hat{\xi}_A^\dagger(0)]\rangle \\ i\Theta(-t)\langle[\hat{\xi}_A(0), \hat{\xi}_A^\dagger(t)]\rangle & 0 \end{pmatrix} \quad (\text{A12})$$

$$\mathbf{G}_C(t) = \begin{pmatrix} -i\langle\{\hat{\xi}_C(t), \hat{\xi}_C^\dagger(0)\}\rangle & -i\Theta(t)\langle[\hat{\xi}_C(t), \hat{\xi}_C^\dagger(0)]\rangle \\ i\Theta(-t)\langle[\hat{\xi}_C(0), \hat{\xi}_C^\dagger(t)]\rangle & 0 \end{pmatrix} \quad (\text{A13})$$

with  $\Theta(t)$  the Heaviside step function,  $\{\cdot, \cdot\}$  the anticommutator and  $[\cdot, \cdot]$  the commutator respectively. Here, the bath operators are in the Heisenberg picture generated by their free evolution, and the expectation values are taken with respect a stationary-state of each bath, which is what allowed us to assume that  $\mathbf{G}_A$  and  $\mathbf{G}_C$  only depend on the difference between  $t$  and  $t'$ . This transformation does not change the functional measure of the baths fields and, more importantly, leads to an action in which the baths are uncoupled from the system of interest. The oscillator degrees of freedom can then be integrated out exactly, leaving us with an action that describes only the qubit and cavity. Due to the linear transformations Eqs. (A10) and (A11) and the coupling term Eqs. (A8) and (A9), however, the system action acquires an additional term that is nonlocal in time and take the form

$$- \int_{-\infty}^{\infty} dt \int_{-\infty}^{\infty} dt' (\mathbf{a}^\dagger(t) \Sigma_a(t-t') \mathbf{a}(t) + \mathbf{c}^\dagger(t) \Sigma_c(t-t') \mathbf{c}(t)) \quad (\text{A14})$$

where the qubit and cavity self energy are directly related to the bath's Green's functions:

$$\Sigma_a(t) = \kappa_a \sigma_x \mathbf{G}_A(t) \sigma_x \equiv \begin{pmatrix} 0 & \Sigma_a^A(t) \\ \Sigma_a^R(t) & \Sigma_a^K(t) \end{pmatrix} \quad (\text{A15})$$

$$\Sigma_c(t) = \kappa_c \sigma_x \mathbf{G}_C(t) \sigma_x \equiv \begin{pmatrix} 0 & \Sigma_c^A(t) \\ \Sigma_c^R(t) & \Sigma_c^K(t) \end{pmatrix} \quad (\text{A16})$$

where  $\Sigma_{a/c}^A(t)$ ,  $\Sigma_{a/c}^R(t)$  and  $\Sigma_{a/c}^K(t)$  are the advanced, retarded and Keldysh component of the self-energy respectively. The first two capture the response properties of the baths. For the linear, Gaussian baths under consideration, these quantities are independent of the state of the baths. Only the Keldysh component of the self-energy carries this information.

To obtain a Markovian description of the dynamics, we assume that the bath density of states of the qubit and cavity are flat. Within this approximation, both  $\hat{\xi}_A(t)$  and  $\hat{\xi}_C(t)$  become the operator equivalent of Gaussian white noise. In particular, the commutator between the bath operators at different times is simply a delta function  $[\hat{\xi}_A(t), \hat{\xi}_A^\dagger(t')] = [\hat{\xi}_C(t), \hat{\xi}_C^\dagger(t')] = \delta(t-t')$ . Physically, since the commutator  $[\hat{\xi}_{A/C}(t), \hat{\xi}_{A/C}^\dagger(t')]$  is directly linked to the linear response properties of the bath via the Kubo formula, this implies that the bath auto-correlation time is vanishingly small. We further assume that the baths are in thermal equilibrium. Since dissipation is weak, we would only be probing frequencies near the resonance frequency of the qubit or cavity. In the spirit of the Markov approximation, we may then set  $\langle \hat{\xi}_{A/C}^\dagger(t) \hat{\xi}_{A/C}(t') \rangle = \delta(t-t') \bar{n}_{a/c}^0$ , where  $\bar{n}_{a/c}^0$  is the thermal occupation number evaluated at the qubit/cavity frequency. We stress that this

is a standard approximation, and is necessary if we want Markovian dynamics.

Using both of these results, the self-energies can then be written as

$$\Sigma_a(t) = -i\kappa_a\delta(t)\begin{pmatrix} 0 & -\Theta(-t) \\ \Theta(t) & (2\bar{n}_a^0 + 1) \end{pmatrix} \quad (\text{A17})$$

$$\Sigma_c(t) - i\kappa_c\delta(t)\begin{pmatrix} 0 & -\Theta(-t) \\ \Theta(t) & (2\bar{n}_c^0 + 1) \end{pmatrix}. \quad (\text{A18})$$

Using the identity

$$\int_{-\infty}^t dt' \delta(t-t') = \frac{1}{2} \quad (\text{A19})$$

we thus arrive at the final system action

$$\begin{aligned} S = & \int_{-\infty}^{\infty} dt \left( a_q^* \left( i\partial_t - \omega_a + i\frac{\kappa_a}{2} \right) a_{cl} + a_{cl}^* \left( i\partial_t - \omega_a - i\frac{\kappa_a}{2} \right) a_q + i\kappa_a (2\bar{n}_a^0 + 1) a_q^* a_q \right. \\ & + \frac{U}{2} (a_q^* a_{cl} + a_{cl}^* a_q) (a_q^* a_q + a_{cl}^* a_{cl}) + g (a_q^* c_{cl} + c_q^* c_{cl} + a_{cl}^* c_q + c_{cl}^* c_q) \\ & \left. + c_q^* \left( i\partial_t - \omega_c + i\frac{\kappa_c}{2} \right) c_{cl} + c_{cl}^* \left( i\partial_t - \omega_c - i\frac{\kappa_c}{2} \right) c_q + i\kappa_c (2\bar{n}_c^0 + 1) c_q^* c_q \right) \end{aligned} \quad (\text{A20})$$

where, for notational compactness, we have suppressed the temporal arguments of the fields.

We now wish to compare this action to the one we would obtain if we started with the master equation Eq. (4) in the main text, which we rewrite here for convenience

$$\begin{aligned} \partial_t \hat{\rho} = & -i[\hat{H}_s, \hat{\rho}] + \kappa_a (\bar{n}_a^0 + 1) \mathcal{D}[\hat{a}_0] \hat{\rho} + \kappa_a \bar{n}_a^0 \mathcal{D}[\hat{a}_0^\dagger] \hat{\rho} \\ & + \kappa_c (\bar{n}_c^0 + 1) \mathcal{D}[\hat{c}_0] \hat{\rho} + \kappa_c \bar{n}_c^0 \mathcal{D}[\hat{c}_0^\dagger] \hat{\rho}. \end{aligned} \quad (\text{A21})$$

One can readily obtain a Keldysh action from a master equation using a standard procedure (see Ref. [33] for a pedagogical review). In short, assuming the operators are normal-ordered, creation or annihilation operators acting on the left or right of the density matrix are associated with a field on forward or backward branch of the contour. After rotating to the classical and quantum basis, the contribution to the action from the dissipation is

$$S_{a,\text{diss}} = \int_{-\infty}^{\infty} dt a^\dagger(t) \begin{pmatrix} 0 & -i\frac{\kappa_a}{2} \\ i\frac{\kappa_a}{2} & i\kappa_a (2\bar{n}_a^0 + 1) \end{pmatrix} a(t) \quad (\text{A22})$$

$$S_{c,\text{diss}} = \int_{-\infty}^{\infty} dt c^\dagger(t) \begin{pmatrix} 0 & -i\frac{\kappa_c}{2} \\ i\frac{\kappa_c}{2} & i\kappa_c (2\bar{n}_c^0 + 1) \end{pmatrix} c(t). \quad (\text{A23})$$

In addition to the contribution to the action from the coherent Hamiltonian, the total Keldysh action is in fact Eq. (A5). The upshot is then that the two theories are equivalent, as promised. The only approximations we have made are standard ones, namely that the cavity and qubit baths are independent and Markovian.

We briefly note that the same equation (4) can be reproduced from an alternative approach, namely, by constructing Heisenberg-Langevin equations for the system operators  $\hat{a}$  and  $\hat{c}$  [31] by writing down the equation of motion of those operators. By moving to the Heisenberg picture, one can then derive, in a standard manner, the starting master equation Eq. (4) [34]. We note, however, that the advantage of the above Keldysh approach is that we can readily extend our theory to systems, which do not have Markovian baths. This will be briefly addressed in the next subsection.

## 2. Beyond the Markovian approximation — Coherent drive case

Here, we will extend the result presented in the last section of the main text by relaxing the assumption that the bath density of states of the cavity is completely flat. This, in turn, implies that the self-energies are no longer frequency independent. For clarity of presentation, we will assume that the qubit is not explicitly coupled to a thermal bath: the only loss it experiences is through its interaction with the cavity. We note that we can easily extend this result to the case where the intrinsic qubit decay rate is large.

Without the Markovian assumption, it is convenient to express the action in frequency space. The quadratic part of the action then takes the form

$$\int_{-\infty}^{\infty} \frac{d\omega}{2\pi} (a_{cl}^* \ c_{cl}^* \ a_q^* \ c_q^*) \mathbf{G}_0^{-1}[\omega] \begin{pmatrix} a_{cl} \\ c_{cl} \\ a_q \\ c_q \end{pmatrix} \quad (\text{A24})$$

where the free Green's function is given by

$$\mathbf{G}_0^{-1}[\omega] = \begin{pmatrix} 0 & (\mathbf{G}_0^{-1}[\omega])^A \\ (\mathbf{G}_0^{-1}[\omega])^R & (\mathbf{G}_0^{-1}[\omega])^K \end{pmatrix} \quad (\text{A25})$$

with

$$(\mathbf{G}_0^{-1}[\omega])^R = (\mathbf{G}_0^{-1}[\omega])^A \dagger = \begin{pmatrix} \omega - \omega_A & -g \\ -g & \omega - \omega_c - \Sigma_c^R[\omega] \end{pmatrix} \quad (\text{A26})$$

$$(\mathbf{G}_0^{-1}[\omega])^K = \begin{pmatrix} 0 & 0 \\ 0 & -\Sigma_c^K[\omega] \end{pmatrix}. \quad (\text{A27})$$

Here, we have suppressed the frequency dependence of the fields for notational simplicity. The retarded and Keldysh part of the self-energy is

$$\Sigma_c^R[\omega] = -\frac{i}{2} \kappa_c [\omega] \quad (\text{A28})$$

$$\Sigma_c^K[\omega] = -i\kappa_c [\omega] (2\bar{n}_c[\omega] + 1). \quad (\text{A29})$$

Without a flat density of states, the self-energies are frequency-dependent and, consequently, we obtain a theory that is nonlocal in time.

We can however still make progress by assuming that  $\kappa_c[\omega]$  is smooth and a slow-varying function of frequency. In this case, it is best to diagonalize the quadratic coherent problem

$$(\mathbf{G}_0^{-1}[\omega])^R = \begin{pmatrix} \omega - \tilde{\omega}_a - \Sigma_c^R[\omega] \frac{g^2}{\Delta^2} & -\Sigma_c^R[\omega] \frac{g}{\Delta} \\ -\Sigma_c^R[\omega] \frac{g}{\Delta} & \omega - \tilde{\omega}_c - \Sigma_c^R[\omega] \left(1 - \frac{g^2}{\Delta^2}\right) \end{pmatrix} \quad (\text{A30})$$

$$(\mathbf{G}_0^{-1}[\omega])^K = -\Sigma_c^K[\omega] \begin{pmatrix} \frac{g^2}{\Delta^2} & \frac{g}{\Delta} \\ \frac{g}{\Delta} & 1 - \frac{g^2}{\Delta^2} \end{pmatrix} \quad (\text{A31})$$

where, as in the main text, we have ignored terms of order  $g^3/\Delta^3$ . The off-diagonal elements of these matrices correspond to dissipation induced coupling between the polaritons (because they are proportional to the self energies).

In the penultimate section of the main text, we considered how the presence of coherent photons modified the  $T_1$ -decay rate of the qubit. We found that the largest contribution to the change in the decay rate does not come from these off-diagonal terms: we can thus safely ignore them. Within this approximation, the quadratic part of the action is thus diagonal in the polariton basis. We may then apply the Markovian approximation to each polariton separately: since dissipation is weak and  $\Sigma_c^R[\omega]$  and  $\Sigma_c^K[\omega]$  are slowly varying functions of  $\omega$ , the largest contribution to the frequency integral will be near  $\tilde{\omega}_a$  or  $\tilde{\omega}_c$  depending on which polariton we are concerned with. Under this approximation, the Green's function now take the form

$$(\mathbf{G}_0^{-1}[\omega])^R = \begin{pmatrix} \omega - \tilde{\omega}_a + i \frac{\kappa_c[\tilde{\omega}_a]}{2} \frac{g^2}{\Delta^2} & 0 \\ 0 & \omega - \tilde{\omega}_c + i \frac{\kappa_c[\tilde{\omega}_c]}{2} \left(1 - \frac{g^2}{\Delta^2}\right) \end{pmatrix} \quad (\text{A32})$$

$$(\mathbf{G}_0^{-1}[\omega])^K = \begin{pmatrix} i\kappa_c[\tilde{\omega}_a] (2\bar{n}_c[\tilde{\omega}_a]) \frac{g^2}{\Delta^2} & 0 \\ 0 & i\kappa_c[\tilde{\omega}_c] (2\bar{n}_c[\tilde{\omega}_c] + 1) \left(1 - \frac{g^2}{\Delta^2}\right) \end{pmatrix}. \quad (\text{A33})$$

Once this replacement has been made, the analysis of the coherently driven circuit is nearly identical. The upshot is then that the second main result, Eq. (20) still holds with the replacement

$$\tilde{\kappa}_a \rightarrow \frac{g^2}{\Delta^2} \kappa_c[\tilde{\omega}_a]. \quad (\text{A34})$$

We briefly note that, for the thermal case, the non-Markovian bath extension does not seem straightforward, as the off-diagonal term corresponding to the correlated dissipation plays crucial role there. This issue is left as our future work.

### APPENDIX B: LINDBLAD PERTURBATION THEORY

As its use is not widespread, we briefly outline here the basics of the Lindblad perturbation theory used in the main text, following Refs. [18,19]. Within this framework, the original Lindbladian  $\mathcal{L}$  is split into nonperturbative ( $\mathcal{L}_0$ ) and perturbative ( $\mathcal{L}_1$ ) parts,  $\mathcal{L} = \mathcal{L}_0 + \epsilon \mathcal{L}_1$ ;  $\epsilon = 1$  is introduced as a book-keeping constant. The eigenvalues  $\lambda_\alpha$  and right eigenvectors  $\hat{r}_\alpha$  of  $\mathcal{L}$  are defined via

$$\mathcal{L} \hat{r}_\alpha = \lambda_\alpha \hat{r}_\alpha. \quad (\text{B1})$$

As is done in standard Rayleigh-Schrödinger perturbation theory [35], we write these quantities as a formal power series in  $\epsilon$ :  $\lambda_\alpha = \sum_{j=0}^{\infty} \epsilon^j \lambda_\alpha^{(j)}$  and  $\hat{r}_\alpha = \sum_{j=0}^{\infty} \epsilon^j \hat{r}_\alpha^{(j)}$ . Comparing order by order, we obtain the recursive relation

$$(\mathcal{L}_0 - \lambda_\alpha^{(0)}) \hat{r}_\alpha^{(j)} = -\mathcal{L}_1 \hat{r}_\alpha^{(j-1)} + \sum_{k=1}^j \lambda_\alpha^{(k)} \hat{r}_\alpha^{(j-k)}. \quad (\text{B2})$$

From this relation at  $j = 1$ ,

$$(\mathcal{L}_0 - \lambda_\alpha^{(0)}) \hat{r}_\alpha^{(1)} = -\mathcal{L}_1 \hat{r}_\alpha^{(0)} + \lambda_\alpha^{(1)} \hat{r}_\alpha^{(0)}, \quad (\text{B3})$$

by moving to a basis polaritons. After this transformation, the (inverse) Green's function in this basis take the form

we get the first-order correction to the eigenvalue,

$$\lambda_\alpha^{(1)} = \langle \hat{l}_\alpha^{(0)}, \mathcal{L}_1 \hat{r}_\alpha^{(0)} \rangle. \quad (\text{B4})$$

Here, we have introduced the left eigenstate of the nonperturbative part  $\mathcal{L}_0$  defined as  $\mathcal{L}_0^\dagger \hat{l}_\alpha^{(0)} = \lambda_\alpha^{(0)*} \hat{l}_\alpha^{(0)}$  where  $\mathcal{L}_0^\dagger$  is the adjoint of the Liouvillian superoperator [18]. We have also used  $\langle \hat{l}_\alpha^{(0)}, \hat{r}_\beta^{(0)} \rangle = \delta_{\alpha,\beta}$  with  $\langle \hat{A}, \hat{B} \rangle = \text{tr}[\hat{A}^\dagger \hat{B}]$ .

The first-order correction to the right eigenstate is given by

$$(\mathcal{L}_0 - \lambda_\alpha^{(0)}) \hat{r}_\alpha^{(1)} = -\sum_{\beta \neq \alpha} \hat{r}_\beta^{(0)} \langle \hat{l}_\beta^{(0)}, \mathcal{L}_1 \hat{r}_\alpha^{(0)} \rangle. \quad (\text{B5})$$

Projection to the state  $\beta \neq \alpha$  gives

$$(\lambda_\beta^{(0)} - \lambda_\alpha^{(0)}) \langle \hat{l}_\beta^{(0)}, \hat{r}_\alpha^{(1)} \rangle = -\langle \hat{l}_\beta^{(0)}, \mathcal{L}_1 \hat{r}_\alpha^{(0)} \rangle. \quad (\text{B6})$$

Assuming that the spectrum of the unperturbed Lindbladian is non-degenerate, we have

$$\langle \hat{l}_\beta^{(0)}, \hat{r}_\alpha^{(1)} \rangle = -\frac{\langle \hat{l}_\beta^{(0)}, \mathcal{L}_1 \hat{r}_\alpha^{(0)} \rangle}{\lambda_\beta^{(0)} - \lambda_\alpha^{(0)}}. \quad (\beta \neq \alpha) \quad (\text{B7})$$

Assuming further that  $\{\hat{r}_\alpha^{(0)}\}$  gives a complete set, which is equivalent to assuming that the Lindbladian  $\mathcal{L}^{(0)}$  is diagonalizable (which is always true in our problem), we get the first-order correction to the eigenstates,

$$\hat{r}_\alpha^{(1)} = -\sum_{\beta \neq \alpha} \hat{r}_\beta^{(0)} \frac{\langle \hat{l}_\beta^{(0)}, \mathcal{L}_1 \hat{r}_\alpha^{(0)} \rangle}{\lambda_\beta^{(0)} - \lambda_\alpha^{(0)}}. \quad (\text{B8})$$

Without loss of generality, we have chosen to set  $\langle \hat{l}_\alpha^{(0)}, \hat{r}_\alpha^{(1)} \rangle = 0$ .

Then, using Eq. (B2) for  $j = 2$ ,

$$(\mathcal{L}_0 - \lambda_\alpha^{(0)}) \hat{r}_\alpha^{(2)} = -\mathcal{L}_1 \hat{r}_\alpha^{(1)} + \lambda_\alpha^{(1)} \hat{r}_\alpha^{(1)} + \lambda_\alpha^{(2)} \hat{r}_\alpha^{(0)} \quad (\text{B9})$$

the second-order correction to the eigenvalue is given by

$$\lambda_\alpha^{(2)} = \langle \hat{\rho}_\alpha^{(0)}, \mathcal{L}_1 \hat{\rho}_\alpha^{(1)} \rangle = - \sum_{\beta \neq \alpha} \frac{\langle \hat{\rho}_\alpha^{(0)}, \mathcal{L}_1 \hat{\rho}_\beta^{(0)} \rangle \langle \hat{\rho}_\beta^{(0)}, \mathcal{L}_1 \hat{\rho}_\alpha^{(0)} \rangle}{\lambda_\beta^{(0)} - \lambda_\alpha^{(0)}} \quad (\text{B10})$$

which is our central relation we will use in the following. We note in passing the similarity to usual second-order perturbation theory with the left and right eigenstates replacing the usual orthogonal eigenvectors of a Hermitian Hamiltonian.

### APPENDIX C: THERMAL OCCUPATION

We show here how Lindblad perturbation theory leads to Eq. (14) in the main text for the qubit  $T_1$  decay in the presence of thermal excitations; this perturbative expression is valid for small thermal occupancy in the dispersive limit  $g/|\Delta| \ll 1$ . We will give more quantitative constraints on the validity of our perturbative expansion in what follows.

As done in the main text, we regard the decoupled system

$$\mathcal{L}_0 \hat{\rho} \equiv -i[\hat{H}_s^{(0)}, \hat{\rho}] + \tilde{\kappa}_c((1 + \tilde{n}_c)\mathcal{D}[\hat{c}]\hat{\rho} + \tilde{n}_c\mathcal{D}[\hat{c}^\dagger]\hat{\rho}) + \tilde{\kappa}_a((1 + \tilde{n}_a)\mathcal{D}[\hat{a}]\hat{\rho} + \tilde{n}_a\mathcal{D}[\hat{a}^\dagger]\hat{\rho}) \quad (\text{C1})$$

as the nonperturbative part, where

$$\hat{H}_s^{(0)} = \hat{H}_0 + \hat{H}_{\text{int}}^{\text{slf}} = \tilde{\omega}_c \hat{c}^\dagger \hat{c} + \tilde{\omega}_a \hat{a}^\dagger \hat{a} + \chi_{aa} \hat{a}^\dagger \hat{a}^\dagger \hat{a} \hat{a}. \quad (\text{C2})$$

We treat the remaining part,

$$\mathcal{L}_1 \hat{\rho} \equiv [\mathcal{L} - \mathcal{L}_0] \hat{\rho} = -i[\epsilon_{\text{crs}} \hat{H}_{\text{int}}^{\text{crs}} + \epsilon_{\text{ns}} \hat{H}_{\text{int}}^{\text{nc}}, \hat{\rho}] + \epsilon_{\text{cd}} \mathcal{L}_{\text{cd}} \hat{\rho}, \quad (\text{C3})$$

as a perturbation that is at most  $\mathcal{O}(g/\Delta)$ .

#### 1. Characterization of the non-perturbative part $\mathcal{L}_0$

As is clear from Eq. (B10), the first step in our approach is to characterize the spectral properties of the unperturbed Lindbladian  $\mathcal{L}_0$  (which includes the qubit self-Kerr interaction). Since the cavity and qubit photons are completely decoupled in  $\mathcal{L}_0 = \mathcal{L}_0^c \otimes \hat{1} + \hat{1} \otimes \mathcal{L}_0^a$ , the unperturbed eigenstates have a direct product structure:  $\hat{\rho}_{\alpha_c, \alpha_a}^{(0)} = \hat{\rho}_{\alpha_c}^{(0)} \otimes \hat{\rho}_{\alpha_a}^{(0)}$ ,  $\hat{\rho}_{\alpha_c, \alpha_a}^{(0)} = \hat{\rho}_{\alpha_c}^{(0)} \otimes \hat{\rho}_{\alpha_a}^{(0)}$ . Here, the cavity-photon part of the right eigenstates are right eigenstates of a thermal harmonic oscillator Lindbladian,

$$\begin{aligned} \mathcal{L}_0^c \hat{\rho}_{\alpha_c}^{(0)} &= -i[\tilde{\omega}_c \hat{c}^\dagger \hat{c}, \hat{\rho}_{\alpha_c}^{(0)}] \\ &\quad + \tilde{\kappa}_c((1 + \tilde{n}_c)\mathcal{D}[\hat{c}]\hat{\rho}_{\alpha_c}^{(0)} + \tilde{n}_c\mathcal{D}[\hat{c}^\dagger]\hat{\rho}_{\alpha_c}^{(0)}) \\ &= \lambda_{\alpha_c}^{c(0)} \hat{\rho}_{\alpha_c}^{(0)}, \end{aligned} \quad (\text{C4})$$

and similarly, the right eigenvalues of the qubit satisfy

$$\begin{aligned} \mathcal{L}_0^a \hat{\rho}_{\alpha_a}^{(0)} &= -i[\tilde{\omega}_a \hat{a}^\dagger \hat{a} + \chi_{aa} \hat{a}^\dagger \hat{a}^\dagger \hat{a} \hat{a}, \hat{\rho}_{\alpha_a}^{(0)}] \\ &\quad + \tilde{\kappa}_a((1 + \tilde{n}_a)\mathcal{D}[\hat{a}]\hat{\rho}_{\alpha_a}^{(0)} + \tilde{n}_a\mathcal{D}[\hat{a}^\dagger]\hat{\rho}_{\alpha_a}^{(0)}) \\ &= \lambda_{\alpha_a}^{a(0)} \hat{\rho}_{\alpha_a}^{(0)}. \end{aligned} \quad (\text{C5})$$

The eigenvalue of  $\mathcal{L}_0$  corresponding to  $\hat{\rho}_{\alpha_c, \alpha_a}^{(0)}$  is given by  $\lambda_{\alpha_c, \alpha_a}^{(0)} = \lambda_{\alpha_c}^{c(0)} + \lambda_{\alpha_a}^{a(0)}$ .

It is instructive to point out that  $\mathcal{L}_0^c$  and  $\mathcal{L}_0^a$  commutes with the superoperator  $\mathcal{M}_{c\bullet} = [\hat{c}^\dagger \hat{c}, \bullet]$  and  $\mathcal{M}_{a\bullet} = [\hat{a}^\dagger \hat{a}, \bullet]$ , respectively. One can readily verify that the spectrum of  $\mathcal{M}_a$  and  $\mathcal{M}_c$  consist of the integers  $m_a, m_c \in \mathbb{Z}$ , and each of

these eigenvalues are infinitely degenerate: any outer product of Fock states constitutes an eigenvector. The corresponding eigenvalue is simply the photon number in the ket state minus the photon number in the bra state. Using the familiar result from linear algebra that any two commuting operators share a set of eigenvectors, we conclude that the cavity (qubit) part of the Lindbladian  $\mathcal{L}_0$  takes on a block-diagonal form  $\mathcal{L}_0^{c(a)} = \otimes_{m=-\infty}^{\infty} \mathcal{L}_{0m}^{c(a)}$  [27], where  $\mathcal{L}_{0m}^{c(a)}$  only acts on the eigensubspace of  $\mathcal{M}_{c(a)}$  characterized by the integer eigenvalue  $m$ . In other words,  $m$  is a good quantum number we may use to label our eigenstates. Although this block-diagonal decomposition greatly simplifies our problem, it is worth pointing out that each block is still infinite in size.

Our task now reduces to diagonalizing each superoperator  $\mathcal{L}_{0m}^\mu$ . We may write down the eigenvalue problem as

$$\mathcal{L}_{0m}^\mu \hat{\rho}_{k,m}^{\mu(0)} = \lambda_{k,m}^{\mu(0)} \hat{\rho}_{k,m}^{\mu(0)}. \quad (\text{C6})$$

with the constraint that  $\hat{\rho}_{k,m}^{\mu(0)}$  must be an eigenvector of  $\mathcal{M}_\mu$  with eigenvalue  $m$ . It must then necessarily take the form

$$\hat{\rho}_{k,m}^{\mu(0)} = \begin{cases} \sum_{n=0}^{\infty} r_{k,m,n}^{\mu(0)} |(n+m)_\mu\rangle \langle n_\mu| & m \geq 0 \\ \sum_{n=0}^{\infty} r_{k,m,n}^{\mu(0)} |n_\mu\rangle \langle (n-m)_\mu| & m < 0 \end{cases} \quad (\text{C7})$$

where  $|n_{c(a)}\rangle$  is the Fock state for the cavity (qubit). A similar relation holds for the left eigenstates,

$$\mathcal{L}_{0m}^{\mu\dagger} \hat{\rho}_{k,m}^{\mu(0)*} = \lambda_{k,m}^{\mu(0)*} \hat{\rho}_{k,m}^{\mu(0)*} \quad (\text{C8})$$

with

$$\hat{\rho}_{k,m}^{\mu(0)} = \begin{cases} \sum_{n=0}^{\infty} l_{k,m,n}^{\mu(0)} |(n+m)_\mu\rangle \langle n_\mu| & m \geq 0 \\ \sum_{n=0}^{\infty} l_{k,m,n}^{\mu(0)} |n_\mu\rangle \langle (n-m)_\mu| & m < 0 \end{cases} \quad (\text{C9})$$

We may now, in a very precise way, identify the unperturbed  $T_1$  modes we discussed in the main text: they correspond to eigenmodes labeled by  $m = 0$ . The right and left eigenvectors of these modes only involve Fock-state projectors, and hence only describe the decay of Fock-state populations. In contrast, we refer to states labeled by  $m \neq 0$  as  $T_2$  modes: these necessarily involve decay of off-diagonal elements of the density matrix in the Fock basis. We also point out that the (unique) unperturbed steady-state is necessarily a  $T_1$  mode, i.e., there are no steady-state Fock-state coherences.

We now look into the specific form of the eigenstates. We first consider the  $m = 0$  sector of each respective species, i.e., the steady states and the  $T_1$ -decay modes for the cavity and qubit. Substituting Eq. (C7) at  $m = 0$  into Eqs. (C4) and (C5) (and similarly for the left eigenstates), one finds that the two equations can be collectively described as ( $\mu = c, a$ ),

$$\begin{aligned} \lambda_{k,m=0}^{\mu(0)} r_{k,m=0,n}^{\mu(0)} &= \tilde{\kappa}_\mu [(1 + \tilde{n}_\mu)(n+1)r_{k,m=0,n+1}^{\mu(0)} \\ &\quad - (n + 2\tilde{n}_\mu + \tilde{n}_\mu)r_{k,m=0,n}^{\mu(0)} + \tilde{n}_\mu r_{k,m=0,n-1}^{\mu(0)}], \end{aligned} \quad (\text{C10})$$

or

$$\mathbf{M} \mathbf{r}_{k,m=0}^{\mu(0)} = \lambda_{k,m=0}^{\mu(0)} \mathbf{r}_{k,m=0}^{\mu(0)}, \quad \mathbf{r}_{k,m=0}^{\mu(0)} = \begin{pmatrix} r_{k,m=0,n=0}^{\mu(0)} \\ r_{k,m=0,n=1}^{\mu(0)} \\ r_{k,m=0,n=2}^{\mu(0)} \\ r_{k,m=0,n=3}^{\mu(0)} \\ \vdots \end{pmatrix}, \quad (C11)$$

$$(\mathbf{l}_{k,m=0}^{\mu(0)})^\top \mathbf{M} = \lambda_{k,m=0}^{\mu(0)} (\mathbf{l}_{k,m=0}^{\mu(0)})^\top, \quad \mathbf{l}_{k,m=0}^{\mu(0)} = \begin{pmatrix} l_{k,m=0,n=0}^{\mu(0)} \\ l_{k,m=0,n=1}^{\mu(0)} \\ l_{k,m=0,n=2}^{\mu(0)} \\ l_{k,m=0,n=3}^{\mu(0)} \\ \vdots \end{pmatrix}, \quad (C12)$$

with

$$\mathbf{M} = \tilde{\kappa}_\mu \begin{pmatrix} -\tilde{n}_\mu & 1 + \tilde{n}_\mu & 0 & 0 & 0 & \cdots \\ \tilde{n}_\mu & -1 - 3\tilde{n}_\mu & 2(1 + \tilde{n}_\mu) & 0 & 0 & \cdots \\ 0 & 2\tilde{n}_\mu & -(2 + 5\tilde{n}_\mu) & 3(1 + \tilde{n}_\mu) & 0 & \cdots \\ 0 & 0 & 3\tilde{n}_\mu & -(3 + 7\tilde{n}_\mu) & 4(1 + \tilde{n}_\mu) & \cdots \\ \vdots & \vdots & \vdots & \vdots & \ddots & \vdots \end{pmatrix}. \quad (C13)$$

Note that by definition, the  $m = 0$  modes consist of a linear combination of Fock state projectors. Since the coherent Hamiltonian is diagonal in the Fock basis, it follows that it does not affect these modes at all.

This eigenvalue problem is known to be exactly solvable [26,36], where the eigenvalues are given by

$$\lambda_{k,m=0}^{\mu(0)} = -k\tilde{\kappa}_\mu. \quad (k = 0, 1, 2, \dots) \quad (C14)$$

$k = 0$  corresponds to the steady state solution, while  $k \geq 1$  are the  $T_1$ -decay modes. Remarkably, the eigenvalues are *independent* of thermal occupancy  $\tilde{n}_\mu$ .

While there are many  $T_1$ -decay modes, we are especially interested in the *slowest* mode that describes qubit population decay ( $k = 1$  for qubit) *without* cavity decay ( $k = 0$  for cavity). This eigenvectors of this mode have the form

$$\hat{\mathbf{r}}_{\text{rel}}^{(0)} \equiv \hat{\mathbf{r}}_{\alpha_c=(k=0,m=0),\alpha_a=(k=1,m=0)}^{(0)} \\ = \hat{\mathbf{r}}_{k=0,m=0}^{c(0)} \otimes \hat{\mathbf{r}}_{k=1,m=0}^{a(0)} \equiv \hat{\rho}_{\text{ss}}^{c(0)} \otimes \hat{\mathbf{r}}_{\text{rel}}^{a(0)}, \quad (C15)$$

$$\hat{\mathbf{l}}_{\text{rel}}^{(0)} \equiv \hat{\mathbf{l}}_{\alpha_c=(k=0,m=0),\alpha_a=(k=1,m=0)}^{(0)} \\ = \hat{\mathbf{l}}_{k=0,m=0}^{c(0)} \otimes \hat{\mathbf{l}}_{k=1,m=0}^{a(0)} \equiv \hat{\mathbf{l}}_{\text{ss}}^{c(0)} \otimes \hat{\mathbf{l}}_{\text{rel}}^{a(0)}, \quad (C16)$$

where  $\hat{\mathbf{l}}_{\text{ss}}^{c(0)} = \hat{\mathbf{I}}$  is the left eigenstate of the steady state. We will refer to this mode as the ‘‘qubit  $T_1$ -decay mode’’ and its eigenvalue

$$\Gamma_{\text{rel}}^{(0)} = -\lambda_{k=1,m=0}^{a(0)} = \tilde{\kappa}_a \quad (C17)$$

as the ‘‘qubit  $T_1$ -decay rate’’ [Eq. (13) in the main text]. The other  $T_1$  modes (labelled by  $k \geq 2$ ) will be referred to as ‘‘higher-order qubit  $T_1$  modes’’.

The explicit form of the qubit  $T_1$ -decay mode [Eq. (C15)] is listed below for the latter use. For the cavity part, the steady state  $\hat{\rho}_{\text{ss}}^{c(0)} \equiv \sum_{n=0}^\infty P_{\text{ss},n}^{c(0)} |n_c\rangle \langle n_c|$  is given by

$$P_{\text{ss},n}^{c(0)} = \frac{1}{1 + \tilde{n}_c} \left( \frac{\tilde{n}_c}{1 + \tilde{n}_c} \right)^n, \quad (C18)$$

with the corresponding left eigenstate  $\hat{\mathbf{l}}_{\text{ss}}^{c(0)} = \hat{\mathbf{I}}$ , and the qubit part is given by

$$r_{\text{rel},n}^{a(0)} \equiv r_{k=1,m=0,n}^{a(0)} = -\frac{n - \tilde{n}_a}{1 + \tilde{n}_a} \left( \frac{\tilde{n}_a}{1 + \tilde{n}_a} \right)^{n-1} \quad (C19)$$

and

$$l_{\text{rel},n}^{a(0)} \equiv l_{k=1,m=0,n}^{a(0)} = \frac{-n + \tilde{n}_a}{(1 + \tilde{n}_a)^2}. \quad (C20)$$

In contrast to the  $T_1$ -decay modes, the  $T_2$ -decay modes are affected by the coherent dynamics. Therefore, the Kerr nonlinearity  $\chi_{aa} \sim -U/2$  of the qubit does play a role, and describing the eigenstates and eigenvalues of these modes requires some care.

Let us start with the cavity part where such nonlinearities are absent. These can be computed exactly using the formalism of third quantization [36,37], where the  $T_2$ -decay rates are given by [24,26],

$$\lambda_{k,m}^{c(0)} = -im\tilde{\omega}_c - \frac{\tilde{\kappa}_c}{2} (|m| + 2k). \quad (C21)$$

The corresponding right and left eigenstate for  $k = 0$  and  $m = \pm 1$  (which will be used in later sections) has the form [26]

$$\hat{\mathbf{r}}_{\uparrow}^{c(0)} \equiv \hat{\mathbf{r}}_{k=0,m=1}^{c(0)} \\ = \sum_{n=1}^\infty \left( \frac{\tilde{n}_c}{1 + \tilde{n}_c} \right)^{n-1} \sqrt{n} |n_c\rangle \langle (n-1)_c|, \quad (C22)$$

$$\hat{\mathbf{r}}_{\downarrow}^{c(0)} \equiv \hat{\mathbf{r}}_{k=0,m=-1}^{c(0)} \\ = \sum_{n=1}^\infty \left( \frac{\tilde{n}_c}{1 + \tilde{n}_c} \right)^{n-1} \sqrt{n} |(n-1)_c\rangle \langle n_c|, \quad (C23)$$

and

$$\hat{\mathbf{l}}_{\uparrow}^{c(0)} \equiv \hat{\mathbf{l}}_{k=0,m=1}^{c(0)} = \sum_{n=1}^\infty \frac{\sqrt{n}}{1 + \tilde{n}_c} |n_c\rangle \langle (n-1)_c|, \quad (C24)$$

$$\hat{\Gamma}_{\downarrow}^{c(0)} \equiv \hat{\Gamma}_{k,m=-1}^{c(0)} = \sum_{n=1}^{\infty} \frac{\sqrt{n}}{1+\tilde{n}_c} |(n-1)_c\rangle \langle n_c|, \quad (\text{C25})$$

respectively.

We now turn to the qubit part. As stressed earlier, the nonlinearity plays a role for the  $T_2$ -decay modes and rates, but surprisingly, this problem is known to be exactly solvable [24,25]. We will however not make use of the known exact solution and instead take advantage of the fact that most of the experiments are done in the regime  $U \gg \tilde{\kappa}_a$ ; this leads to a massive simplification. In this regime, the dissipation can be treated perturbatively: the right and left eigenvectors are simply outer products of Fock states [27]. Note crucially that this is only true of the  $T_2$ -decay modes. The  $T_1$ -decay modes are completely insensitive to the coherent dynamics and thus dissipation completely determines the structure of the eigenvectors, as seen above. Keeping this in mind, after a straightforward calculation, we arrive at the perturbative eigenvalue of the  $T_2$   $m = \pm 1$  modes [27]

$$\lambda_{(k+m,m)}^{a(0)} \equiv \lambda_{k,m=\pm 1}^{a(0)} = -im(\tilde{\omega}_a - Uk) - \frac{\tilde{\kappa}_a}{2} [\tilde{n}_a(2k+3) + (1+\tilde{n}_a)(2k+1)], \quad (\text{C26})$$

where we have used the relation  $\chi_{aa} \simeq -U/2$ .

## 2. Derivation of Eq. (14)

We are now in the position to derive the photon dependence to the qubit  $T_1$ -decay rate  $\Gamma_{\text{rel}}$  [Eq. (14) in the main text] in the full problem characterized by the Lindbladian  $\mathcal{L}$  [Eq. (5)]. This is defined, within the second-order perturbation, as the sum of the contribution from the unperturbed  $\Gamma_{\text{rel}}^{(0)}$  [defined in Eq. (C17)] and the perturbative correction to this mode:

$$\Gamma_{\text{rel}} = \Gamma_{\text{rel}}^{(0)} + \Gamma_{\text{rel}}^{(1)} + \Gamma_{\text{rel}}^{(2)}, \quad (\text{C27})$$

Therefore, the leading contribution is from the second-order correction, which is composed of three terms,

$$\begin{aligned} \Gamma_{\text{rel}}^{(2)} &= \sum_{\beta \neq \text{rel}} \left[ \epsilon_{\text{nc}}^2 \frac{\langle \hat{\Gamma}_{\text{rel}}^{(0)}, \mathcal{L}_{\text{nc}} \hat{r}_{\beta}^{(0)} \rangle \langle \hat{\Gamma}_{\beta}^{(0)}, \mathcal{L}_{\text{nc}} \hat{r}_{\text{rel}}^{(0)} \rangle}{\lambda_{\beta}^{(0)} - \lambda_{\text{rel}}^{(0)}} + \epsilon_{\text{cd}}^2 \frac{\langle \hat{\Gamma}_{\text{rel}}^{(0)}, \mathcal{L}_{\text{cd}} \hat{r}_{\beta}^{(0)} \rangle \langle \hat{\Gamma}_{\beta}^{(0)}, \mathcal{L}_{\text{cd}} \hat{r}_{\text{rel}}^{(0)} \rangle}{\lambda_{\beta}^{(0)} - \lambda_{\text{rel}}^{(0)}} \right. \\ &\quad \left. + \epsilon_{\text{nc}} \epsilon_{\text{cd}} \left[ \frac{\langle \hat{\Gamma}_{\text{rel}}^{(0)}, \mathcal{L}_{\text{nc}} \hat{r}_{\beta}^{(0)} \rangle \langle \hat{\Gamma}_{\beta}^{(0)}, \mathcal{L}_{\text{cd}} \hat{r}_{\text{rel}}^{(0)} \rangle}{\lambda_{\beta}^{(0)} - \lambda_{\text{rel}}^{(0)}} + \frac{\langle \hat{\Gamma}_{\text{rel}}^{(0)}, \mathcal{L}_{\text{cd}} \hat{r}_{\beta}^{(0)} \rangle \langle \hat{\Gamma}_{\beta}^{(0)}, \mathcal{L}_{\text{nc}} \hat{r}_{\text{rel}}^{(0)} \rangle}{\lambda_{\beta}^{(0)} - \lambda_{\text{rel}}^{(0)}} \right] \right] \\ &\equiv \epsilon_{\text{nc}}^2 \Gamma_{\text{rel}}^{\text{nc-nc}(2)} + \epsilon_{\text{cd}}^2 \Gamma_{\text{rel}}^{\text{cd-cd}(2)} + \epsilon_{\text{nc}} \epsilon_{\text{cd}} \Gamma_{\text{rel}}^{\text{nc-cd}(2)}. \end{aligned} \quad (\text{C34})$$

The second term  $\Gamma_{\text{rel}}^{\text{cd-cd}(2)}$  can be safely neglected in the regime of our interest  $\kappa_c, \kappa_a \ll U, |\Delta|$  since they would only give contributions  $\propto \kappa_{\mu}^2$ .

We first consider the first term  $\propto \epsilon_{\text{nc}}^2$ , that arises from the second-order process involving nonlinear conversion  $\hat{H}_{\text{int}}^{\text{nc}}$ . This is composed of two processes  $\hat{H}_{\text{int}}^{\text{nc}} = \hat{H}_{c \rightarrow a}^{\text{nc}} + \hat{H}_{a \rightarrow c}^{\text{nc}}$ ;  $\hat{H}_{c \rightarrow a}^{\text{nc}} = \chi_{ca} \hat{a}^{\dagger} \hat{a}^{\dagger} \hat{a} \hat{c}$  that converts the cavity excitation to the qubit excitation and  $\hat{H}_{a \rightarrow c}^{\text{nc}} = \chi_{ca} \hat{c}^{\dagger} \hat{a}^{\dagger} \hat{a} \hat{a}$  is its inverse process. When these two processes act on the qubit  $T_1$ -decay mode  $\hat{r}_{\text{rel}}^{(0)}$ , the resulting states  $\hat{H}_{c \rightarrow a}^{\text{nc}} \hat{r}_{\text{rel}}^{(0)}$  (and  $\hat{r}_{\text{rel}}^{(0)} \hat{H}_{c \rightarrow a}^{\text{nc}}$ ),  $\hat{H}_{a \rightarrow c}^{\text{nc}} \hat{r}_{\text{rel}}^{(0)}$  (and  $\hat{r}_{\text{rel}}^{(0)} \hat{H}_{a \rightarrow c}^{\text{nc}}$ ) will overlap with the  $T_2$ -decay modes,

$$\hat{r}_{\downarrow, (n_a+1, n_a)}^{(0)} \equiv \hat{r}_{\downarrow}^{c(0)} \otimes \hat{r}_{(n_a+1, n_a)}^{a(0)} \quad \text{and} \quad \hat{r}_{\uparrow, (n_a-1, n_a)}^{(0)} \equiv \hat{r}_{\uparrow}^{c(0)} \otimes \hat{r}_{(n_a-1, n_a)}^{a(0)}, \quad (\text{C35})$$

$$\begin{aligned} \text{where } \Gamma_{\text{rel}}^{(1)} &= -\lambda_{\text{rel}}^{(1)} = -\langle \hat{\Gamma}_{\text{rel}}^{(0)}, \mathcal{L}_1 \hat{r}_{\text{rel}}^{(0)} \rangle \text{ and} \\ \Gamma_{\text{rel}}^{(2)} &= -\lambda_{\text{rel}}^{(2)} = \sum_{\beta \neq \text{rel}} \frac{\langle \hat{\Gamma}_{\text{rel}}^{(0)}, \mathcal{L}_1 \hat{r}_{\beta}^{(0)} \rangle \langle \hat{\Gamma}_{\beta}^{(0)}, \mathcal{L}_1 \hat{r}_{\text{rel}}^{(0)} \rangle}{\lambda_{\beta}^{(0)} - \lambda_{\text{rel}}^{(0)}}. \end{aligned} \quad (\text{C28})$$

The perturbative part  $\mathcal{L}_1 = \epsilon_{\text{crs}} \mathcal{L}_{\text{crs}} + \epsilon_{\text{nc}} \mathcal{L}_{\text{nc}} + \epsilon_{\text{cd}} \mathcal{L}_{\text{cd}}$  [Eq. (C3)] is composed of three parts (where  $\epsilon_{\text{crn}} = \epsilon_{\text{nc}} = \epsilon_{\text{cd}} = 1$  are book-keeping constants): cross-Kerr nonlinearity

$$\mathcal{L}_{\text{crs}} \bullet = -i[\hat{H}_{\text{crs}}, \bullet] = -i\chi_{ca} [\hat{c}^{\dagger} \hat{c} \hat{a}^{\dagger} \hat{a}, \bullet], \quad (\text{C29})$$

nonlinear conversion

$$\mathcal{L}_{\text{nc}} \bullet = -i[\hat{H}_{\text{nc}}, \bullet] = -i\tilde{\chi} [\hat{a}^{\dagger} \hat{a}^{\dagger} \hat{a} \hat{c} + \hat{c}^{\dagger} \hat{a}^{\dagger} \hat{a} \hat{a}, \bullet], \quad (\text{C30})$$

and correlated dissipation

$$\begin{aligned} \mathcal{L}_{\text{cd}} \hat{\rho} &= -\frac{1}{2} (\tilde{\gamma}_{\uparrow} + \tilde{\gamma}_{\downarrow}) \{\hat{a}^{\dagger} \hat{c} + \hat{c}^{\dagger} \hat{a}, \hat{\rho}\} \\ &\quad + \tilde{\gamma}_{\downarrow} (\hat{a} \hat{\rho} \hat{c}^{\dagger} + \hat{c} \hat{\rho} \hat{a}^{\dagger}) + \tilde{\gamma}_{\uparrow} (\hat{a}^{\dagger} \hat{\rho} \hat{c} + \hat{c}^{\dagger} \hat{\rho} \hat{a}). \end{aligned} \quad (\text{C31})$$

Let us start by pointing out that the cross-Kerr nonlinearity gives no correction to the qubit  $T_1$ -decay rate  $\Gamma_{\text{rel}}$  to the order of our interest. This is due to the relation

$$\mathcal{L}_{\text{crs}} \hat{r}_{\text{rel}}^{(0)} = \mathcal{L}_{\text{crs}}^{\dagger} \hat{r}_{\text{rel}}^{(0)} = 0, \quad (\text{C32})$$

which follows from the property that the cross-Kerr nonlinearity does not change the number of excitation of each respective species. Therefore, in what follows, we only consider the correction from the nonlinear conversion  $\mathcal{L}_{\text{nc}}$  [Eq. (C30)] and correlated dissipation  $\mathcal{L}_{\text{cd}}$  [Eq. (C31)].

Both of these perturbations  $\mathcal{L}_{\text{nc}}, \mathcal{L}_{\text{cd}}$  involve changes in the number of cavity/qubit excitations, and thus necessarily causes transitions between different eigensubspaces of  $\mathcal{M}_c$  and  $\mathcal{M}_a$ . More prosaically, they couple  $T_1$  modes to  $T_2$  modes and vice versa. From this property, we can immediately conclude that the first-order correction is absent,

$$\Gamma_{\text{rel}}^{(1)} = -\langle \hat{\Gamma}_{\text{rel}}^{(0)}, \mathcal{L}_1 \hat{r}_{\text{rel}}^{(0)} \rangle = 0, \quad (\text{C33})$$

because  $\hat{r}_{\text{rel}}^{(0)}$  and  $\mathcal{L}_1 \hat{r}_{\text{rel}}^{(0)}$  are in different eigensubspaces.

respectively. These have the corresponding eigenvalues

$$\lambda_{\downarrow c, (n_a+1, n_a)}^{(0)} = -\left[\frac{\tilde{\kappa}_c}{2} + \frac{\tilde{\kappa}_a}{2}[\tilde{n}_a(2n_a + 3) + (1 + \tilde{n}_a)(2n_a + 1)]\right] + i[\tilde{\omega}_c - (\tilde{\omega}_a - Un_a)], \quad (C36)$$

$$\lambda_{\uparrow c, (n_a, n_a+1)}^{(0)} = -\left[\frac{\tilde{\kappa}_c}{2} + \frac{\tilde{\kappa}_a}{2}[\tilde{n}_a(2n_a + 3) + (1 + \tilde{n}_a)(2n_a + 1)]\right] - i[\tilde{\omega}_c - (\tilde{\omega}_a - Un_a)], \quad (C37)$$

As a result,  $\Gamma_{\text{rel}}^{\text{nc-nc}(2)}$  is composed of two parts (where we introduce a short-hand notation  $|n_c, n_a\rangle \equiv |n_c\rangle \otimes |n_a\rangle$ ),

$$\begin{aligned} \Gamma_{\text{rel}}^{\text{nc-nc}(2)} &= -\sum_{n_c, n_a=0}^{\infty} p_{\text{ss}, n_c}^{c(0)} r_{\text{rel}, n_a}^{a(0)} \\ &\times \left[ 2\text{Re} \left[ \frac{1}{\tilde{\kappa}_a + \lambda_{\downarrow c, (n_a+1, n_a)}^{(0)}} \right] \text{tr} \left[ \hat{l}_{\text{rel}}^{(0)\dagger} \hat{H}_{a \rightarrow c}^{\text{ns}} \hat{r}_{\downarrow c, (n_a+1, n_a)}^{c(0)} - \hat{l}_{\text{rel}}^{(0)\dagger} \hat{r}_{\downarrow c, (n_a+1, n_a)}^{c(0)} \hat{H}_{a \rightarrow c}^{\text{ns}} \right] \text{tr} \left[ \hat{l}_{\downarrow c, (n_a+1, n_a)}^{(0)\dagger} \hat{H}_{c \rightarrow a}^{\text{ns}} |n_c, n_a\rangle \langle n_c, n_a| \right] \right. \\ &+ 2\text{Re} \left[ \frac{1}{\tilde{\kappa}_a + \lambda_{\uparrow c, (n_a-1, n_a)}^{(0)}} \right] \text{tr} \left[ \hat{l}_{\text{rel}}^{(0)\dagger} \hat{H}_{c \rightarrow a}^{\text{ns}} \hat{r}_{\uparrow c, (n_a-1, n_a)}^{c(0)} - \hat{l}_{\text{rel}}^{(0)\dagger} \hat{r}_{\uparrow c, (n_a-1, n_a)}^{c(0)} \hat{H}_{c \rightarrow a}^{\text{ns}} \right] \text{tr} \left[ \hat{l}_{\uparrow c, (n_a-1, n_a)}^{(0)\dagger} \hat{H}_{a \rightarrow c}^{\text{ns}} |n_c, n_a\rangle \langle n_c, n_a| \right] \left. \right], \\ &= -2\tilde{\chi}^2 \sum_{n_c, n_a=0}^{\infty} p_{\text{ss}, n_c}^{c(0)} r_{\text{rel}, n_a}^{a(0)} \left[ \text{Re} \left[ \frac{1}{\tilde{\kappa}_a + \lambda_{\downarrow c, (n_a+1, n_a)}^{(0)}} \right] n_a C_{n_c}^{c, \text{ss}\downarrow} C_{n_a}^{a, \text{rel}\uparrow} + \text{Re} \left[ \frac{1}{\tilde{\kappa}_a + \lambda_{\uparrow c, (n_a-1, n_a)}^{(0)}} \right] (n_a - 1) C_{n_c}^{c, \text{ss}\uparrow} C_{n_a}^{a, \text{rel}\downarrow} \right], \end{aligned} \quad (C38)$$

where

$$C_{n_c}^{c, \text{ss}\downarrow} = \text{tr} \left[ \hat{l}_{\text{ss}}^{c(0)\dagger} \hat{c}^\dagger \hat{r}_{\downarrow}^{c(0)} - \hat{l}_{\text{ss}}^{c(0)\dagger} \hat{r}_{\downarrow}^{c(0)} \hat{c}^\dagger \right] \text{tr} \left[ \hat{l}_{\downarrow}^{c(0)\dagger} \hat{c} |n_c\rangle \langle n_c| \right] = \frac{n_c}{1 + \tilde{n}_c} \sum_{n'_c=1}^{\infty} \left[ \left( \frac{\tilde{n}_c}{1 + \tilde{n}_c} \right)^{n'_c-1} \frac{n'_c}{1 + \tilde{n}_c} \right] \quad (C39)$$

$$C_{n_c}^{c, \text{ss}\uparrow} = \text{tr} \left[ \hat{l}_{\text{ss}}^{c(0)\dagger} \hat{c} \hat{r}_{\uparrow}^{c(0)} - \hat{l}_{\text{ss}}^{c(0)\dagger} \hat{r}_{\uparrow}^{c(0)} \hat{c} \right] \text{tr} \left[ \hat{l}_{\uparrow}^{c(0)\dagger} \hat{c}^\dagger |n_c\rangle \langle n_c| \right] = \frac{1 + n_c}{1 + \tilde{n}_c} \sum_{n'_c=0}^{\infty} \left[ \left( \frac{\tilde{n}_c}{1 + \tilde{n}_c} \right)^{n'_c} \frac{1 + n'_c}{1 + \tilde{n}_c} \right] \quad (C40)$$

$$C_{n_a}^{a, \text{rel}\downarrow} = \text{tr} \left[ \hat{l}_{\text{rel}}^{a(0)\dagger} \hat{a}^\dagger \hat{r}_{(n_a-1, n_a)}^{a(0)} - \hat{l}_{\text{rel}}^{a(0)\dagger} \hat{r}_{(n_a-1, n_a)}^{a(0)} \hat{a}^\dagger \right] \text{tr} \left[ \hat{l}_{(n_a-1, n_a)}^{a(0)\dagger} \hat{a} |n_a\rangle \langle n_a| \right] = \text{tr} \left[ \hat{l}_{\text{rel}}^{a(0)\dagger} \mathcal{D}[\hat{a}] (|n_a\rangle \langle n_a|) \right] \quad (C41)$$

$$C_{n_a}^{a, \text{rel}\uparrow} = \text{tr} \left[ \hat{l}_{\text{rel}}^{a(0)\dagger} \hat{a} \hat{r}_{(n_a+1, n_a)}^{a(0)} - \hat{l}_{\text{rel}}^{a(0)\dagger} \hat{r}_{(n_a+1, n_a)}^{a(0)} \hat{a} \right] \text{tr} \left[ \hat{l}_{(n_a+1, n_a)}^{a(0)\dagger} \hat{a}^\dagger |n_a\rangle \langle n_a| \right] = \text{tr} \left[ \hat{l}_{\text{rel}}^{a(0)\dagger} \mathcal{D}[\hat{a}^\dagger] (|n_a\rangle \langle n_a|) \right]. \quad (C42)$$

At the low temperature regime  $\tilde{n}_c^0, \tilde{n}_a^0 \ll 1$ , it is sufficient to sum up the first several Fock states,

$$\begin{aligned} \Gamma_{\text{rel}}^{\text{nc-nc}(2)} &\approx -\tilde{\chi}^2 \frac{\tilde{\kappa}_a + \tilde{\kappa}_c}{(\Delta - U)^2} \left[ p_{\text{ss}, n_c=1}^{c(0)} r_{\text{rel}, n_a=1}^{a(0)} C_{n_c=1}^{c, \text{ss}\downarrow} C_{n_a=1}^{a, \text{rel}\uparrow} + p_{\text{ss}, n_c=0}^{c(0)} r_{\text{rel}, n_a=2}^{a(0)} C_{n_c=0}^{c, \text{ss}\uparrow} C_{n_a=2}^{a, \text{rel}\downarrow} \right] \\ &\approx -\frac{g^2 U^2}{\Delta^2} \frac{\tilde{\kappa}_a + \tilde{\kappa}_c}{(\Delta - U)^2} (2\tilde{n}_c - 4\tilde{n}_a) \end{aligned} \quad (C43)$$

giving the third term of Eq. (14) in the main text.

Equation (C43) tells us that, for the contribution solely from nonlinear conversion, increasing the qubit thermal population  $\tilde{n}_a$  increases the qubit  $T_1$ -decay rate. In contrast, increasing cavity thermal population  $\tilde{n}_c$  decreases this rate. Note that the former can be important even when the bare qubit population is absent ( $\tilde{n}_a^0 = 0, \tilde{n}_c^0 > 0$ ) in the regime  $\kappa_a \ll \kappa_p$ , as the qubit population can be comparable to the cavity population  $\tilde{n}_a \simeq \tilde{n}_c$ , see Eq. (8) in the main text. This intriguing property can be understood by using Fermi's Golden rule: There is an effective incoherent pumping or decay process between the qubit  $n = 1$  and  $n = 2$  Fock state mediated by the cavity. (Note crucially that the excitations between  $n = 0$  and  $n = 1$  qubit Fock state is absent because the nonlinear conversion can only take place when at least one qubit photon present.) To see this, it is instructive to rewrite Eq. (C43) as

$$\Gamma_{\text{rel}}^{\text{nc-nc}(2)} \approx -\left( \hat{l}_{\text{rel}}^{a(0)\dagger}, \mathcal{L}_{\text{eff}}^{\text{nc}} \hat{r}_{\text{rel}}^{a(0)} \right) \quad (C44)$$

with

$$\mathcal{L}_{\text{eff}}^{\text{nc}} = \kappa_{\text{eff}}^{\text{nc}} (\tilde{n}_c \mathcal{D}[\hat{a}_{n \geq 1}^\dagger] + \mathcal{D}[\hat{a}_{n \geq 2}]), \quad (C45)$$

$$\kappa_{\text{eff}}^{\text{nc}} = \tilde{\chi}^2 \frac{\tilde{\kappa}_a + \tilde{\kappa}_c}{(\Delta - U)^2}, \quad (C46)$$

where we have introduced annihilation/creation operators  $\hat{a}_{n \geq 2}$  and  $\hat{a}_{n \geq 1}^\dagger$  that only acts on higher-number Fock states, i.e.,

$$\hat{a}_{n \geq 2} |n\rangle = \sqrt{n} |n-1\rangle, \quad \hat{a}_{n \geq 1}^\dagger |n\rangle = \sqrt{n+1} |n+1\rangle \quad (C47)$$

but  $\hat{a}_{n \geq 2} |n\rangle = 0 (n \leq 1)$ ,  $\hat{a}_{n \geq 1}^\dagger |n\rangle = 0 (n = 0)$ , reflecting the absence of the excitations between  $n = 0$  and  $n = 1$  states from the nonlinear conversion process.

The fact that  $\Gamma_{\text{rel}}^{\text{rel}(2)}$  can be expressed as Eqs. (C44) and (C45) shows that  $\Gamma_{\text{rel}}^{\text{nc-nc}(2)}$  can be interpreted as a first-order

correction from the effective dissipator  $\mathcal{L}_{\text{eff}}^{\text{nc}}$  [cf. Eq. (B4)]. The effective dissipation rate  $\kappa_{\text{eff}}^{\text{nc}}$  [Eq. (C46)] can be understood as the Fermi's Golden rule rate of the transition from the  $(n_c, n_a) = (1, 1)$  state to  $(n_c, n_a) = (0, 2)$  state (and its inverse), where it is given as the product of the transition rate  $\tilde{\chi}^2$  and the density of states. The first term of  $\mathcal{L}_{\text{eff}}^{\text{nc}}$  that describes the effective incoherent qubit pumping process from qubit  $n = 1$  to  $n = 2$  state is proportional to  $\tilde{n}_c$  because the nonlinear conversion that excites the qubit can only activate in the presence of the cavity photon population. This incoherent pumping process to the higher qubit states contributes as the *decrease* of the qubit  $T_1$ -decay rate, which follows from the relation  $\langle \hat{r}_{\text{rel}}^{a(0)}, \mathcal{D}[\hat{a}_{n \geq 1}^\dagger] \hat{r}_{\text{rel}}^{a(0)} \rangle \approx 2$ . Note that the fact that this involves the  $n = 2$  qubit Fock state is essential in obtaining

the negative contribution to  $\Gamma_{\text{rel}}$ , since the transition between  $n = 0$  and  $n = 1$  would affect the  $T_1$ -decay rate in the opposite way, following from  $\langle \hat{r}_{\text{rel}}^{a(0)}, \mathcal{D}[\hat{a}^\dagger] \hat{r}_{\text{rel}}^{a(0)} \rangle \approx -1$  at low temperature.

On the other hand, its inverse process from the qubit  $n = 2$  to  $n = 1$  state contribute as the increase of the qubit  $T_1$ -decay rate. Since the  $n = 2$  state can only be populated when the qubit is populated ( $\tilde{n}_a > 0$ ), this term is proportional to  $\tilde{n}_a$ , which follows from the relation  $\langle \hat{r}_{\text{rel}}^{a(0)}, \mathcal{D}[\hat{a}_{n \geq 2}] \hat{r}_{\text{rel}}^{a(0)} \rangle \approx -4\tilde{n}_a$ .

We can similarly compute the third term  $\Gamma_{\text{rel}}^{\text{nc-cd}(2)}$  of Eq. (C34), which is the ‘‘cross term’’ contribution of the nonlinear conversion and correlated dissipation. As in the first term  $\Gamma_{\text{rel}}^{\text{nc-nc}(2)}$ , the intermediate states are given by Eq. (C35). After a lengthy but straightforward computation, we arrive at

$$\begin{aligned} \Gamma_{\text{rel}}^{\text{nc-cd}(2)} &= \sum_{n_c, n_a=0}^{\infty} p_{ss, n_c}^{c(0)} r_{\text{rel}, n_a}^{a(0)} \\ &\times \left[ 2\tilde{\gamma}_\downarrow \tilde{\chi} \text{Im} \left[ \frac{1}{\tilde{\kappa}_a + \lambda_{\downarrow, c, (n_a, n_a-1)}^{(0)}} \right] (n_a - 1) C_{n_c}^{c, ss\downarrow} C_{n_a}^{a, \text{rel}\downarrow} + 2\tilde{\gamma}_\downarrow \tilde{\chi} \text{Im} \left[ \frac{1}{\tilde{\kappa}_a + \lambda_{\uparrow, c, (n_a-1, n_a)}^{(0)}} \right] (n_a - 1) C_{n_c}^{c, ss\uparrow} C_{n_a}^{a, \text{rel}\uparrow} \right. \\ &\left. + 2\tilde{\gamma}_\uparrow \tilde{\chi} \text{Im} \left[ \frac{1}{\tilde{\kappa}_a + \lambda_{\uparrow, c, (n_a, n_a+1)}^{(0)}} \right] n_a C_{n_c}^{c, ss\uparrow} C_{n_a}^{a, \text{rel}\uparrow} + 2\tilde{\gamma}_\uparrow \tilde{\chi} \text{Im} \left[ \frac{1}{\tilde{\kappa}_a + \lambda_{\downarrow, c, (n_a+1, n_a)}^{(0)}} \right] n_a C_{n_c}^{c, ss\downarrow} C_{n_a}^{a, \text{rel}\downarrow} \right]. \end{aligned} \quad (\text{C48})$$

A notable difference from Eq. (C38) is that the *imaginary* part of the ‘‘propagator’’  $G_\beta = 1/(-\tilde{\kappa}_a - \lambda_\beta^{(0)})$  (where  $\beta$  labels the intermediate state) enters the expression, while the *real* part of  $G_\beta$  shows up in Eq. (C38). The physical meaning of the latter is the density of states of the system, while the former is related to that by the Kramers-Kronig relation. This difference reflects the property that this term originates from the combination of the coherent and dissipative perturbation. Comparing the relation  $\text{Im}G_\beta \sim 1/(\Delta - U)$  and  $\text{Re}G_\beta \sim \tilde{\kappa}_{c,a}/(\Delta - U)^2$ , one finds that this gives rise to one factor of  $\Delta - U$  larger compared to  $\Gamma_{\text{rel}}^{\text{nc-nc}(2)}$  and the peculiar sign dependence to the sign of  $\Delta - U$ . Indeed, at low temperature  $n_c^0, n_a^0 \ll 1$ , we find

$$\begin{aligned} \Gamma_{\text{rel}}^{\text{nc-cd}(2)} &\approx 2\tilde{\gamma}_\downarrow \tilde{\chi} \frac{-1}{\Delta - U} p_{ss, n_c=0}^{c(0)} r_{\text{rel}, n_a=2}^{a(0)} C_{n_c=0}^{c, ss\uparrow} C_{n_a=2}^{a, \text{rel}\downarrow} + 2\tilde{\gamma}_\uparrow \tilde{\chi} \frac{-1}{\Delta - U} p_{ss, n_c=0}^{c(0)} r_{\text{rel}, n_a=1}^{a(0)} C_{n_c=0}^{c, ss\downarrow} C_{n_a=1}^{a, \text{rel}\uparrow} \\ &\approx 2\tilde{\gamma}_\downarrow \tilde{\chi} \frac{-1}{\Delta - U} \langle \hat{r}_{\text{rel}}^{a(0)} \mathcal{D}[\hat{a}_{n \geq 2}] \hat{r}_{\text{rel}}^{a(0)} \rangle + 2\tilde{\gamma}_\uparrow \tilde{\chi} \frac{-1}{\Delta - U} \langle \hat{r}_{\text{rel}}^{a(0)} \mathcal{D}[\hat{a}_{n \geq 1}^\dagger] \hat{r}_{\text{rel}}^{a(0)} \rangle \\ &\approx 2(\kappa_c - \kappa_a) \frac{g^2 U}{\Delta^2} \frac{-1}{\Delta - U} (-4\tilde{n}_a) + 2(\kappa_c \tilde{n}_c^0 - \kappa_a \tilde{n}_a^0) \frac{g^2 U}{\Delta^2} \frac{-1}{\Delta - U} \cdot 2 \\ &= \frac{g^2}{\Delta^2} \frac{U}{\Delta - U} [8(\kappa_c - \kappa_a) \tilde{n}_a - 4(\kappa_c \tilde{n}_c^0 - \kappa_a \tilde{n}_a^0)], \end{aligned} \quad (\text{C49})$$

giving the second term of Eq. (14). Note crucially that, again, the transition between  $(n_c, n_a) = (1, 1)$  Fock state to  $(n_c, n_a) = (0, 2)$  state and its inverse is playing the dominant role to this term as well, as one can see from the second line of Eq. (C49).

This completes the derivation of Eq. (14).

### 3. Limitation of Eq. (14)

So far, we have analytically derived the second-order corrections to the qubit  $T_1$ -decay rate  $\Gamma_{\text{rel}}$  in terms of the nonlinear conversion and correlated dissipation  $\mathcal{L}_1$ . As seen in Figs. 2 and 3 in the main text, the obtained formula [Eq. (14) in the main text] gives an excellent agreement with our numerical simulation (which we provide details in Appendix E) in most regimes. However, we see a slight deviation when

the nonlinearity is relatively large  $U = 0.1|\Delta|$  and is in the regime where the qubit decay  $\tilde{\kappa}_a$  is dominated by Purcell decay contribution  $\kappa_a \ll \kappa_P$ . Notably, the formula recovers its predictive power in the opposite regime  $\kappa_a > \kappa_P$ , even with large nonlinearity  $U = 0.1|\Delta|$ , see Fig. 3.

We argue below that this deviation is due to the missing higher-order correction in terms of  $\mathcal{L}_1$ , that can become important when  $\kappa_a \ll \kappa_P$ . We show that there exists correction to  $\Gamma_{\text{rel}}$  of  $\mathcal{O}((g^2 U^2 / \Delta^4) \kappa_c \tilde{n}_c)$  from the higher-order perturbation *only* in the regime  $\kappa_a \ll \kappa_P$ , which is comparable to  $\Gamma_{\text{rel}}^{\text{nc-nc}(2)}$  [the third term of Eq. (14) in the main text]. This is due to the appearance of ‘‘resonant’’ processes that involves higher order qubit  $T_1$ -decay modes as its intermediate state. These results are in agreement with what is seen in the numerics. We stress, however, that the qualitative features and the order of magnitude of the correction are well captured already in Eq. (14),

since the most dominant correction of  $\mathcal{O}((g^2U/\Delta^3)\kappa_\mu\tilde{n}_\mu)$  from the second term of Eq. (14) is already appropriately included in our second-order perturbation theory.

The next-order correction would be from the fourth-order perturbation in terms of  $\mathcal{L}_1$ . From the recursion relation (B2), we have

$$\begin{aligned}\Gamma_{\text{rel}}^{(4)} &= -\langle \hat{l}_{\text{rel}}^{(0)}, \mathcal{L}_1 \hat{r}_{\text{rel}}^{(3)} \rangle = -\langle \hat{l}_{\text{rel}}^{(0)}, \mathcal{L}_1 (\mathcal{L}_0 + \tilde{\kappa}_a)^{-1} \mathcal{L}_1 (\mathcal{L}_0 + \tilde{\kappa}_a)^{-1} \mathcal{L}_1 (\mathcal{L}_0 + \tilde{\kappa}_a)^{-1} \mathcal{L}_1 \hat{r}_{\text{rel}}^{(0)} \rangle \\ &= -\sum_{\mu=\text{crs,nc,cd}} \sum_{\beta,\gamma,\delta \neq \text{rel}} \langle \hat{l}_{\text{rel}}^{(0)}, \mathcal{L}_1^\mu \hat{r}_\beta^{(0)} \rangle \frac{1}{\lambda_\beta^{(0)} + \tilde{\kappa}_a} \langle \hat{l}_\beta, \mathcal{L}_1^\mu \hat{r}_\gamma^{(0)} \rangle \frac{1}{\lambda_\gamma^{(0)} + \tilde{\kappa}_a} \langle \hat{l}_\gamma^{(0)}, \mathcal{L}_1^\mu \hat{r}_\delta^{(0)} \rangle \frac{1}{\lambda_\delta^{(0)} + \tilde{\kappa}_a} \langle \hat{l}_\delta^{(0)}, \mathcal{L}_1^\mu \hat{r}_{\text{rel}}^{(0)} \rangle\end{aligned}\quad (\text{C50})$$

where we have introduced a compact notation for the cross-Kerr nonlinearity  $\mathcal{L}_1^{\mu=\text{crs}} = \mathcal{L}_{\text{crs}}$ , nonlinear conversion  $\mathcal{L}_1^{\mu=\text{nc}} = \mathcal{L}_{\text{nc}}$ , and correlated dissipation  $\mathcal{L}_1^{\mu=\text{cd}} = \mathcal{L}_{\text{cd}}$ . As in Rayleigh-Schrödinger perturbation theory for quantum mechanics, this can be understood as a result of the summation over all possible processes involving four steps of virtual excitations from the unperturbed initial state.

Let us consider in particular the process where two nonlinear conversion ( $\mathcal{L}_{\text{nc}}$ ) and two correlated dissipation ( $\mathcal{L}_{\text{cd}}$ ) are involved, which evolves the qubit  $T_1$ -decay mode as follows:

$$\hat{r}_{\text{rel}}^{(0)} \xrightarrow{\mathcal{L}_{\text{nc}}} \hat{r}_\delta = \hat{r}_\downarrow^{c(0)} \otimes \hat{r}_{(n_a+1, n_a)}^{a(0)} \xrightarrow{\mathcal{L}_{\text{cd}}} \hat{r}_\gamma = \hat{\rho}_{\text{ss}}^{c(0)} \otimes \hat{r}_{k=2, m=0}^{a(0)} \xrightarrow{\mathcal{L}_{\text{nc}}} \hat{r}_\beta = \hat{r}_\downarrow^{c(0)} \otimes \hat{r}_{(n_a+1, n_a)}^{a(0)} \xrightarrow{\mathcal{L}_{\text{cd}}} \hat{r}_{\text{rel}}^{(0)}.\quad (\text{C51})$$

Here,  $n_a$  only takes  $n_a \geq 1$  because the nonlinear conversion only activates when qubit excitation is present. This is a process where the qubit  $T_1$ -decay mode is excited to a  $T_2$  mode by the nonlinear conversion  $\mathcal{L}_{\text{nc}}$ , then converted to a *higher order* qubit  $T_1$ -decay mode by the correlated dissipation  $\mathcal{L}_{\text{cd}}$ , and then ultimately transferring back to the qubit  $T_1$ -decay mode by the further perturbation from  $\mathcal{L}_{\text{nc}}$  and  $\mathcal{L}_{\text{cd}}$ . The contribution from this process can be estimated as

$$\begin{aligned}\Gamma_{\text{rel}}^{(4)} &\sim \tilde{\chi}^2 \tilde{\gamma}_\uparrow^2 P_{\text{ss}, n_c=1}^{c(0)} r_{\text{rel}, n_a=1}^{a(0)} \text{Re} \left[ \frac{1}{\lambda_{\downarrow c, (n_a=2, n_a=1)}^{(0)} + \tilde{\kappa}_a} \frac{1}{\lambda_{k=2, m=0}^{a(0)} + \tilde{\kappa}_a} \frac{1}{\lambda_{\downarrow c, (n_a=2, n_a=1)}^{(0)} + \tilde{\kappa}_a} \right] \\ &\sim \tilde{\chi}^2 \tilde{\gamma}_\uparrow^2 \tilde{n}_c \frac{1}{(\Delta - U)^2} \frac{1}{\tilde{\kappa}_a} \simeq \frac{g^4}{\Delta^4} \frac{U^2}{(\Delta - U)^2} \frac{(\kappa_c - \kappa_a)^2}{\tilde{\kappa}_a} \tilde{n}_c\end{aligned}\quad (\text{C52})$$

at low temperature. Here, it is proportional to  $\tilde{\chi}^2 \tilde{\gamma}_\uparrow^2$  because two nonlinear conversion and correlated dissipation are involved, and have used Eqs. (C14) and (C36) to estimate the contribution from the propagators of the intermediate states.

Due to the fact that this is a contribution from the fourth-order correction,  $\Gamma_{\text{rel}}^{(4)}$  is proportional to  $g^4/\Delta^4$ . This, at a glance, seems to always give only subleading-order correction to  $\Gamma_{\text{rel}}$  compared to the corrections given in Eq. (14) in the main text that are  $\propto g^2/\Delta^2$ . However, note the appearance of the qubit decay rate  $\tilde{\kappa}_a$  in the *denominator* in its expression, which is due to the property that this process involves a (higher order) qubit  $T_1$ -decay mode as its intermediate state. Because of this “resonant” structure, in the regime  $\kappa_a \ll \kappa_P = (g^2/\Delta^2)(\kappa_c - \kappa_a)$ , we can further estimate the correction as (recall that  $\tilde{\kappa}_a = \kappa_a + \kappa_P \simeq \kappa_P$  in this regime)

$$\begin{aligned}\Gamma_{\text{rel}}^{(4)} &\sim \frac{g^4}{\Delta^4} \frac{U^2}{(\Delta - U)^2} \frac{\kappa_c^2}{\frac{g^2}{\Delta^2}(\kappa_c - \kappa_a)} \tilde{n}_c \\ &\sim \frac{g^2}{\Delta^2} \frac{U^2}{(\Delta - U)^2} \kappa_c \tilde{n}_c,\end{aligned}\quad (\text{C53})$$

which is comparable to the third term in Eq. (14) in the main text. Note how one of the  $g^2/\Delta^2$  factor in the numerator is canceled out with that in the denominator to yield this large magnitude. The obtained order of magnitude matches with the magnitude of the deviation between Eq. (14) and the numerics. This is also consistent with the observation made in Fig. 2 in the main text that Eq. (14) matches with the numerics

at very small  $U \ll |\Delta|$ , where the second term of Eq. (14) dominates over  $\Gamma_{\text{rel}}^{(4)}$ .

On the other hand, when  $\kappa_a \gg \kappa_P$ ,  $\tilde{\kappa}_a$  in the denominator of Eq. (C52) does not get as small and the cancellization of  $g^2/\Delta^2$  seen above does not occur. As a result,  $\Gamma_{\text{rel}}^{(4)} \propto g^4/\Delta^4$  only gives subleading correction compared to the terms obtained in Eq. (14) in the main text. This is consistent with the results obtained in Fig. 3, where an excellent agreement is still obtained even with a relatively large nonlinearity  $U (= 0.1|\Delta|)$ .

#### APPENDIX D: BARE CAVITY COHERENT DRIVE

This section deals with the bare cavity coherent drive  $\hat{H}_D = f_c e^{-i\omega_D t} \hat{c}_0 + \text{H.c.}$  and will derive Eq. (20) in the main text. As sketched in the main text, we first move to the rotating frame that eliminates the time dependence from the Hamiltonian and further make a displacement transformation that eliminates linear terms  $\propto \hat{c}_0, \hat{a}_0$  from the Hamiltonian. The resulting equation of motion at weak drive regime  $|\alpha_a|^2 \ll 1$  and zero temperature  $\bar{n}_c^0 = \bar{n}_a^0 = 0$  is given by,

$$\partial_t \hat{\rho} = -i[\hat{H}'_s, \hat{\rho}] + \kappa_a \mathcal{D}[\hat{a}_0] \hat{\rho} + \kappa_c \mathcal{D}[\hat{c}_0] \hat{\rho} \equiv \mathcal{L}' \hat{\rho}, \quad (\text{D1})$$

with

$$\hat{H}'_s \simeq \hat{H}'_0 + \hat{H}'_{\text{int}}, \quad (\text{D2})$$

where

$$\hat{H}'_0 = \hat{H}_0 + \hat{H}_{\text{quad}}$$

$$\begin{aligned} &\simeq (\omega_a - \omega_D - 2U|\alpha_a|^2)\hat{a}_0^\dagger\hat{a}_0 + g(\hat{a}_0^\dagger\hat{c}_0 + \text{h.c.}) \\ &\quad + (\omega_c - \omega_D)\hat{c}_0^\dagger\hat{c}_0, \end{aligned} \quad (\text{D3})$$

is a *modified* quadratic Hamiltonian from the energy shift that arises due to the drive (where the squeezing terms  $\sim\hat{a}_0\hat{a}_0$  and  $\hat{a}_0^\dagger\hat{a}_0^\dagger$  are omitted as they play no role to the order of our interest), and

$$\hat{H}'_{\text{int}} = \hat{H}_{\text{int}} + \hat{V}[\alpha_a], \quad \hat{V}[\alpha_a] = -U(\alpha_a\hat{a}_0^\dagger\hat{a}_0^\dagger + \text{H.c.}). \quad (\text{D4})$$

The displacement fields  $\alpha_c, \alpha_a$  satisfy the relation,

$$\begin{pmatrix} \omega_c - \omega_D - i\kappa_c/2 & g \\ g & \omega_a - \omega_D - i\kappa_a/2 \end{pmatrix} \begin{pmatrix} \alpha_c \\ \alpha_a \end{pmatrix} = - \begin{pmatrix} f_c \\ 0 \end{pmatrix}.$$

In what follows, we diagonalize the modified quadratic Hamiltonian as  $\hat{H}'_0 = (\tilde{\omega}'_a - \omega_D)\hat{a}'^\dagger\hat{a}' + (\tilde{\omega}'_c - \omega_D)\hat{c}'^\dagger\hat{c}'$  by introducing the modified polariton operators  $\hat{c}' \simeq [1 - g^2/(2\Delta'^2)]\hat{c}_0 - (g/\Delta')\hat{a}_0$  and  $\hat{a}' \simeq [1 - g^2/(2\Delta'^2)]\hat{a}_0 + (g/\Delta')\hat{c}_0$ , where  $\tilde{\omega}'_a \simeq \omega_a + g^2/\Delta'$  and  $\tilde{\omega}'_c \simeq \omega_c + g^2/\Delta'$ . These expressions has the same form as the usual blackbox basis without coherent drive (see main text), where the qubit-cavity detuning  $\Delta = \omega_a - \omega_c$  is replaced by

$$\Delta'[\alpha_a] = \Delta - 2U|\alpha_a|^2, \quad (\text{D5})$$

since the only difference between  $\hat{H}_0$  and  $\hat{H}'_0$  is the energy shift from the drive.

For the interaction term  $\hat{H}'_{\text{int}} \approx \hat{H}'_{\text{int}}{}^{\text{slf}'} + \hat{H}'_{\text{int}}{}^{\text{crs}'} + \hat{H}'_{\text{int}}{}^{\text{nc}'}$ , they are given as the sum of the self- and cross-Kerr nonlinearity and the nonlinear conversion as before [cf. Eqs. (2) and (3) in the main text],

$$\hat{H}'_{\text{int}}{}^{\text{slf}'} = \chi'_{aa}\hat{a}'^\dagger\hat{a}'^\dagger\hat{a}'\hat{a}', \quad (\text{D6})$$

$$\hat{H}'_{\text{int}}{}^{\text{crs}'} = \chi'_{ca}\hat{c}'^\dagger\hat{c}'^\dagger\hat{a}'\hat{a}', \quad (\text{D7})$$

$$\hat{H}'_{\text{int}}{}^{\text{nc}'} = \tilde{\chi}'(\hat{a}'^\dagger\hat{a}'^\dagger\hat{c}'\hat{c}' + \hat{c}'^\dagger\hat{c}'^\dagger\hat{a}'\hat{a}'), \quad (\text{D8})$$

with  $\chi'_{aa} = -(U/2)[1 - g^2/(2\Delta'^2)]$ ,  $\chi'_{ca} = -2g^2U/\Delta'^2$ , and  $\tilde{\chi}' = gU/\Delta'$ . The drive term  $\hat{V}[\alpha_a]$  transforms as

$$\hat{V}[\alpha_a] \approx -U(\alpha_a\hat{a}'^\dagger\hat{a}'^\dagger + \text{H.c.}), \quad (\text{D9})$$

where we have dropped the higher-order corrections  $\mathcal{O}((g^2/\Delta'^2)U\alpha_a, \alpha_a^3)$ .

The resulting Lindblad master equation in this basis takes the form

$$\partial_t\hat{\rho} = \mathcal{L}'\hat{\rho} = \mathcal{L}'_{\text{ind}}\hat{\rho} + \mathcal{L}'_{\text{cd}}\hat{\rho}. \quad (\text{D10})$$

Here,  $\mathcal{L}'_{\text{ind}}$  and  $\mathcal{L}'_{\text{cd}}$  take the similar form to  $\mathcal{L}_{\text{ind}}$  [Eq. (6) in the main text] and  $\mathcal{L}_{\text{cd}}$  [Eq. (9) in the main text], respectively, except for the replacement of parameters and some additional terms arising from the drive  $\hat{V}[\alpha_a]$ :

$$\mathcal{L}'_{\text{ind}}\hat{\rho} = -i[\hat{H}'_s, \hat{\rho}] + \kappa'_a[\alpha_a]\mathcal{D}[\hat{a}']\hat{\rho} + \kappa'_c[\alpha_a]\mathcal{D}[\hat{c}']\hat{\rho} \quad (\text{D11})$$

$$\begin{aligned} \mathcal{L}'_{\text{cd}}\hat{\rho} = & -\frac{\tilde{\gamma}'_{\downarrow}[\alpha_a]}{2}\{\hat{a}'^\dagger\hat{c}' + \hat{c}'^\dagger\hat{a}', \hat{\rho}\} \\ & + \tilde{\gamma}'_{\downarrow}[\alpha_a](\hat{a}'\hat{\rho}\hat{c}'^\dagger + \hat{c}'\hat{\rho}\hat{a}'^\dagger). \end{aligned} \quad (\text{D12})$$

As stressed in the main text, the intrinsic qubit polariton damping rate is modified to

$$\begin{aligned} \tilde{\kappa}'_a[\alpha_a] &= \kappa_a + \frac{g^2}{(\Delta'[\alpha_a])^2}(\kappa_c - \kappa_a) \\ &\simeq \kappa_a + \kappa_P + \frac{g^2}{\Delta^2}\frac{4U}{\Delta}(\kappa_c - \kappa_a)|\alpha_a|^2 \end{aligned} \quad (\text{D13})$$

and similarly for the cavity polariton dissipation rate and correlated dissipation rate,

$$\begin{aligned} \tilde{\kappa}'_c[\alpha_a] &= \kappa_c + \frac{g^2}{(\Delta'[\alpha_a])^2}(\kappa_a - \kappa_c) \\ &\simeq \kappa_c - \kappa_P - \frac{g^2}{\Delta^2}\frac{4U}{\Delta}(\kappa_c - \kappa_a)|\alpha_a|^2, \end{aligned} \quad (\text{D14})$$

$$\tilde{\gamma}'_{\downarrow}[\alpha_a] = \frac{g}{\Delta'[\alpha_a]}(\kappa_c - \kappa_a) \quad (\text{D15})$$

$$\simeq \tilde{\gamma}_{\downarrow} + \frac{2gU}{\Delta}(\kappa_c - \kappa_a)|\alpha_a|^2. \quad (\text{D16})$$

We now compute the qubit  $T_1$ -decay rate  $\Gamma_{\text{rel}}[\alpha_a]$  of this system. Since the form of the master equation (D10) is very much similar to that of the thermal case [Eq. (5) in the main text], most of the analysis below would be parallel to the previous section. Similarly to the thermal case, we regard the qubit-cavity coupling terms and  $\hat{V}[\alpha_a]$  that gives rise to nonsecular nonlinearity, given by

$$\mathcal{L}'_1\hat{\rho} = -i[\epsilon_{\text{crs}}\hat{H}'_{\text{int}}{}^{\text{crs}'} + \epsilon_{\text{ns}}\hat{H}'_{\text{int}}{}^{\text{nc}'} + \epsilon_V\hat{V}[\alpha_a], \hat{\rho}] + \epsilon_{\text{cd}}\mathcal{L}'_{\text{cd}}\hat{\rho} \quad (\text{D17})$$

as the perturbation on top of the unperturbed part  $\mathcal{L}'_0 = \mathcal{L}' - \mathcal{L}'_1$ , or

$$\mathcal{L}'_0\hat{\rho} = -i[\hat{H}'_0 + \hat{H}'_{\text{int}}{}^{\text{slf}'}, \hat{\rho}] + \kappa'_a[\alpha_a]\mathcal{D}[\hat{a}']\hat{\rho} + \kappa'_c[\alpha_a]\mathcal{D}[\hat{c}']\hat{\rho}. \quad (\text{D18})$$

Here, again,  $\epsilon_{\text{crs}} = \epsilon_{\text{ns}} = \epsilon_V = \epsilon_{\text{cd}} = 1$  is the book-keeping constant. We will compute up to the second-order in  $\mathcal{L}'_1$ , where the qubit  $T_1$ -decay rate is given by  $\Gamma_{\text{rel}}[\alpha_a] = \Gamma_{\text{rel}}^{(0)} + \Gamma_{\text{rel}}^{(2)}$ . (The first-order correction vanishes as before.)

The unperturbed part Eq. (D18) has the same form as that of the thermal case Eq. (C1). Therefore, those results can be directly applied by the appropriate replacement of the parameters such as  $\tilde{\kappa}_\mu \rightarrow \tilde{\kappa}'_\mu[\alpha_a]$ . This gives the unperturbed qubit  $T_1$ -decay rate [cf. Eq. (C17)]

$$\Gamma_{\text{rel}}^{(0)}[\alpha_a] = \tilde{\kappa}'_a[\alpha_a] = \kappa_a + \kappa_P + \frac{g^2}{\Delta^2}\frac{4U}{\Delta}(\kappa_c - \kappa_a)|\alpha_a|^2. \quad (\text{D19})$$

Note that the coherent drive strength dependence is already included in this unperturbed part.

We move on to consider the perturbative correction to the qubit  $T_1$ -decay rate from  $\mathcal{L}'_1$ . Actually, it turns out that the only contribution at zero temperature is that from  $\hat{V}[\alpha_a]$ . As before, the cross-Kerr nonlinearity does not contribute to the qubit  $T_1$ -decay rate since they do not change the photon excitation number. For the nonlinear conversion and the correlated dissipation to be activated, photon excitations should be present in the steady state, which, however, are absent at zero temperature  $\bar{n}_c^0 = \bar{n}_a^0 = 0$ .

Since  $\hat{V}[\alpha_a]$  only excites the qubit, the intermediate state that participates to the second-order correction to the qubit  $T_1$ -decay rate would be of the form that solely involves the coherence of the qubit,

$$\hat{r}_{ss,(n_a+1,n_a)}^{(0)} \equiv \hat{\rho}_{ss}^{c(0)} \otimes \hat{r}_{(n_a+1,n_a)}^{a(0)} \quad (D20)$$

$$\begin{aligned} \Gamma_{\text{rel}}^{(2)}[\alpha_a] &\approx -\epsilon_V^2 U^2 |\alpha_a|^2 2\text{Re} \left[ \frac{1}{\tilde{\kappa}_a + \lambda_{ss,(n_a=2,n_a=1)}^{(0)}} \right] \langle \hat{r}_{\text{rel}}^{a(0)}, \mathcal{D}[\hat{a}_{n \geq 1}^\dagger] \hat{r}_{\text{rel}}^{a(0)} \rangle \\ &\approx -\epsilon_V^2 \frac{2U^2}{(\tilde{\omega}_a - \omega_D - U)^2} \tilde{\kappa}_a |\alpha_a|^2, \end{aligned} \quad (D22)$$

where the creation operator  $\hat{a}_{n \geq 1}^\dagger$  only acts on the Fock states with  $n \geq 1$ . It is proportional to  $\tilde{\kappa}_a$  and the denominator has the form  $(\tilde{\omega}_a - \omega_D - U)^2$  [in contrast to Eq. (C43) where it is proportional to  $\tilde{\kappa}_a + \tilde{\kappa}_c$  and  $1/(\Delta - U)^2$ ], reflecting the eigenvalue of the intermediate state. This is the second term of Eq. (20) in the main text and hence completes the derivation.

#### APPENDIX E: NUMERICAL SIMULATION

We outline here the procedure we took to determine the qubit  $T_1$ -decay rate  $\Gamma_{\text{rel}}^{\text{diag}}$  from numerical diagonalization of the Lindbladian both for the thermal case  $\mathcal{L}$  [Eq. (4) in the main text] and  $\mathcal{L}'$  for the coherent drive case [Eq. (D10)]. To identify the qubit  $T_1$ -decay rate, recall that the density matrix evolves as

$$\hat{\rho}(t) = \hat{\rho}_{ss} + \sum_{\alpha} w_{\alpha} e^{\lambda_{\alpha} t} \hat{r}_{\alpha} \quad (E1)$$

with  $w_{\alpha} = \langle \hat{l}_{\alpha}, \hat{\rho}(0) \rangle$ . Here, we took the normalization of  $\hat{r}_{\alpha}$  and  $\hat{l}_{\alpha}$  to satisfy  $\text{Tr}[\hat{l}_{\alpha}^\dagger \hat{l}_{\alpha}] = 1$  together with the bi-orthogonality relation  $\text{Tr}[\hat{l}_{\alpha}^\dagger \hat{r}_{\beta}] = \delta_{\alpha,\beta}$ . Equation (E1) tells us that if one starts in an initial state where the qubit is excited, e.g., by adding a single photon to the steady state

$$\hat{\rho}(0) \propto \hat{a}^\dagger \hat{\rho}_{ss} \hat{a}. \quad (E2)$$

then one will excite a set of Liouvillian eigenmodes  $\hat{r}_{\alpha}$  each with its own exponential decay rate  $-\text{Re} \lambda_{\alpha}$ . We can define operationally the  $T_1$ -decay rate of the qubit by the slowest decay rate associated with such an initial state (as this will define the long-time relaxation). Alternatively, we could define the  $T_1$ -decay rate as the rate associated with the excited mode with the largest weight  $|w_{\alpha}|$  (i.e., the mode that most closely represents the deviation between the initial state and the steady state). Either of these definitions can be used from numerical simulations to extract the qubit  $T_1$  rate; for all parameters shown in our numerical plots, both definitions yield the same result. The resulting numerically-obtained qubit  $T_1$ -decay rate defined as  $\Gamma_{\text{rel}}^{\text{diag}} = -\lambda_{\text{rel}}$  is computed using QuTiP code [28,29] and are plotted in Figs. 1–3 in the main text.

A more direct and experimentally relevant way to compute the  $T_1$ -decay rate is to fit the photon number to an exponentially decaying curve after transient dynamics have damped out. To gain further confidence in our approach, we have also computed the qubit  $T_1$ -decay rate  $\Gamma_{\text{rel}}^{\text{sim}}$  in this manner from

with corresponding eigenvalue

$$\lambda_{ss,(n_a+1,n_a)}^{(0)} = -\frac{\tilde{\kappa}_a}{2}(1 + 2n_a) + i(\tilde{\omega}'_a - \omega_D - Un_a). \quad (D21)$$

As a result, the second-order correction is computed as

the direct simulation of the Lindblad master equation (5) with initial condition given by Eq. (E2). We have fitted the time evolution of the qubit photon number to  $\langle \hat{a}^\dagger \hat{a} \rangle(t) \sim e^{-\Gamma_{\text{rel}}^{\text{sim}} t}$  at long times, and compared  $\Gamma_{\text{rel}}^{\text{diag}}$  and  $\Gamma_{\text{rel}}^{\text{sim}}$  in Fig. 4. As one sees, we find an excellent agreement between the two qubit  $T_1$ -decay rates, supporting our approach of determining  $\Gamma_{\text{rel}}$  numerically.

#### APPENDIX F: EXTENSIONS TO OTHER MODELS - QUBIT-MEDIATED CROSS-KERR INTERACTION

In this section, we briefly explain how our general formalism could be applied to other relevant driven-dissipative circuit QED models studied in the literature. We will not explicitly perform the calculation, but rather setup the problem and sketch the solution so that any interested reader could apply the same technique to their model. We focus on a ubiquitous system studied in the context of bosonic error

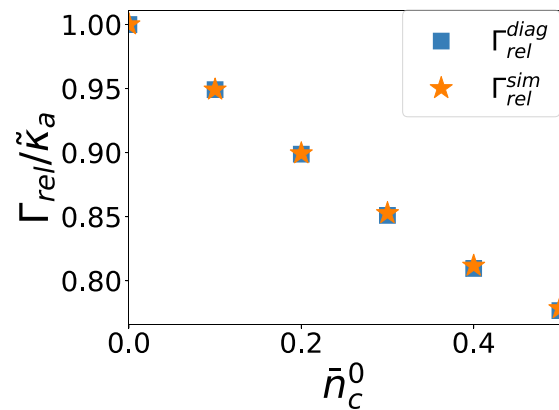


FIG. 4. Comparison between the two different definitions of qubit  $T_1$ -decay rate  $\Gamma_{\text{rel}}^{\text{diag}}$  and  $\Gamma_{\text{rel}}^{\text{sim}}$ . Here,  $\Gamma_{\text{rel}}^{\text{diag}}$  is determined from numerical diagonalization of the Lindbladian  $\mathcal{L}$  (see main text).  $\Gamma_{\text{rel}}^{\text{sim}}$  is determined by numerically computing  $\langle \hat{a}^\dagger \hat{a} \rangle(t)$  and fitting to the relation  $\langle \hat{a}^\dagger \hat{a} \rangle(t) \sim A e^{-\Gamma_{\text{rel}}^{\text{sim}} t}$  at late times. This is computed by simulating Eq. (5) in the main text, with the initial state set to the form of Eq. (E2). For the fitting, we have used the data set at  $t = [0.95T, T]$ , where  $T = 8 \times 10^4 |\Delta|$ . The two different definitions of qubit  $T_1$ -decay rates  $\Gamma_{\text{rel}}^{\text{diag}}$  and  $\Gamma_{\text{rel}}^{\text{sim}}$  are in excellent agreement. We have taken the same parameters as that of Fig. 3(a) (with  $\kappa_a = 0$ ) in the main text.

correction: two (bare) linear cavity modes  $\hat{b}_0$  and  $\hat{c}_0$  are both off-resonantly coupled to a common transmon qubit  $\hat{a}_0$  [38]. The goal here is to use the transmon to mediate nonlinear mode-mode interactions. Of course, an issue is the transmon will also generate unwanted dissipative interactions, which are drive dependent. Our approach provides a powerful means to treat this system.

The starting Hamiltonian describing the isolated system is

$$\begin{aligned} \hat{H}_0 = & \omega_b \hat{b}_0^\dagger \hat{b}_0 + \omega_c \hat{c}_0^\dagger \hat{c}_0 + \omega_a \hat{a}_0^\dagger \hat{a}_0 - \frac{U}{2} \hat{a}_0^\dagger \hat{a}_0^\dagger \hat{a}_0 \hat{a}_0 \\ & + (g_b \hat{a}_0^\dagger \hat{b}_0 + g_c \hat{a}_0^\dagger \hat{c}_0 + f_b e^{-i\omega_D t} \hat{b}_0 + f_c e^{-i\omega_D t} \hat{c}_0 + \text{H.c.}) \end{aligned} \quad (\text{F1})$$

where  $\omega_k$  is the bare resonant frequency,  $g_k$  is the coupling between the linear mode and the qubit, and  $f_k$  the strength of the coherent drive on each linear mode, which we take to be at the same frequency  $\omega_D$ . As we have done throughout, we shall assume that each mode is subject to its own independent Markovian environment with decay rate  $\kappa_{k_0}$  and thermal occupation  $\bar{n}_{k_0}$  for  $k \in \{a, b, c\}$ . Following the procedure outlined in Appendix A, integrating out the Markovian baths leads to the master equation

$$\begin{aligned} \partial_t \hat{\rho} = & -i[\hat{H}_0, \hat{\rho}] \\ & + \sum_{k \in a, b, c} (\kappa_{k_0} (\bar{n}_{k_0} + 1) \mathcal{D}[\hat{k}_0] \hat{\rho} + \kappa_k \bar{n}_{k_0} \mathcal{D}[\hat{k}_0^\dagger] \hat{\rho}), \end{aligned} \quad (\text{F2})$$

which, note, is written in terms of the bare qubit and cavity modes. We can now succinctly outline how to apply our method to this problem, which can be readily generalized to more complicated setups.

(i) First diagonalize the linear and quadratic parts of  $\hat{H}_0$ . This involves moving to a rotating frame at frequency  $\omega_D$ , diagonalizing the quadratic  $3 \times 3$  matrix via a simple unitary transformation and then performing a simple displacement transformation to eliminate the linear drives. With this procedure, one obtains a set of polariton modes  $\hat{k}$ , which, by construction, can be written as a linear combination of the bare modes  $\hat{k}_0$  and the drives  $f_k$ . Given that the detuning between the bare qubit and cavity modes are much larger than their

coupling  $|g_{b/c}/(\omega_a - \omega_{b/c})|^2 \ll 1$ , these polaritons will serve as the starting point for Lindblad perturbation theory.

(ii) One then writes the coherent Hamiltonian  $H_0$  in this new polariton basis. This gives rise to the usual self and cross-Kerr interaction. In addition, to lowest order in  $|g_{b/c}/(\omega_a - \omega_k)|$ , there will be a set of nonlinear conversion processes of the form  $\tilde{\chi}_{b/ca} \hat{a}^\dagger \hat{a}^\dagger \hat{b} \hat{c}$  and  $\alpha_a^* \hat{a}^\dagger \hat{a} \hat{a}$ , where  $\alpha_a$  is proportional to the drive strength. Although they are non-resonant, one must keep these terms since, as explained in the main text, the interplay between the dissipative conversion and this coherent nonlinear conversion will lead to the leading-order correction in the qubit  $T_1$ -decay rate.

(iii) The jump terms are also written in terms of the polariton creation and annihilation operators. Writing these out explicitly, one makes a distinction between the terms, which describe damping of the polariton modes and those which describe a dissipative conversion process. Retaining only the former amounts to making the standard secular approximation; our method relies on keeping all such terms.

(iv) With all relevant terms in hand, one splits the Lindbladian in two parts  $\hat{\mathcal{L}} = \hat{\mathcal{L}}_0 + \hat{\mathcal{L}}_1$ . The first term  $\hat{\mathcal{L}}_0$  consists solely of terms, which do not couple the various polariton modes. We stress that  $\hat{\mathcal{L}}_0$  includes self-Kerr interactions, which (as discussed in the main text) can be treated exactly. The remaining part describes the dissipative and coherent polariton-polariton coupling terms. All such terms are necessarily of the order  $|g_{b/c}/(\omega_a - \omega_{b/c})|$  (assuming  $|g_b/(\omega_a - \omega_b)| \sim |g_c/(\omega_a - \omega_c)|$ ) and thus serve as the correct starting point for Lindblad perturbation theory.

(v) The eigenvalues and eigenvectors of  $\hat{\mathcal{L}}_0$  must then be found, usually within some approximate scheme (using e.g. the smallness of the bare nonlinearity  $U$ ). This only involves solving three single-mode problems, since  $\hat{\mathcal{L}}_0$  does not couple the different polaritons. This was done explicitly in Appendices C and D.

(vi) One can now perform Lindblad perturbation in  $\hat{\mathcal{L}}_1$  using  $\hat{\mathcal{L}}_0$  as the unperturbed Lindbladian. With this information, one can systematically investigate, e.g., how qubit-induced dissipation depends on drive amplitudes and the strength of the various thermal noise terms.

- 
- [1] A. Blais, R.-S. Huang, A. Wallraff, S. M. Girvin, and R. J. Schoelkopf, Cavity quantum electrodynamics for superconducting electrical circuits: An architecture for quantum computation, *Phys. Rev. A* **69**, 062320 (2004).
- [2] A. Blais, A. L. Grimsmo, S. M. Girvin, and A. Wallraff, Circuit quantum electrodynamics, *Rev. Mod. Phys.* **93**, 025005 (2021).
- [3] A. Blais, S. M. Girvin, and W. D. Oliver, Quantum information processing and quantum optics with circuit quantum electrodynamics, *Nat. Phys.* **16**, 247 (2020).
- [4] A. A. Houck, H. E. Türeci, and J. Koch, On-chip quantum simulation with superconducting circuits, *Nat. Phys.* **8**, 292 (2012).
- [5] I. Carusotto, A. A. Houck, A. J. Kollár, P. Roushan, D. I. Schuster, and J. Simon, Photonic materials in circuit quantum electrodynamics, *Nat. Phys.* **16**, 268 (2020).
- [6] M. Boissonneault, J. M. Gambetta, and A. Blais, Dispersive regime of circuit QED: Photon-dependent qubit dephasing and relaxation rates, *Phys. Rev. A* **79**, 013819 (2009).
- [7] C. M. Wilson, G. Johansson, T. Duty, F. Persson, M. Sandberg, and P. Delsing, Dressed relaxation and dephasing in a strongly driven two-level system, *Phys. Rev. B* **81**, 024520 (2010).
- [8] F. Beaudoin, J. M. Gambetta, and A. Blais, Dissipation and ultrastrong coupling in circuit qed, *Phys. Rev. A* **84**, 043832 (2011).
- [9] E. A. Sete, J. M. Gambetta, and A. N. Korotkov, Purcell effect with microwave drive: Suppression of qubit relaxation rate, *Phys. Rev. B* **89**, 104516 (2014).
- [10] M. Fitzpatrick, N. M. Sundaresan, A. C. Y. Li, J. Koch, and A. A. Houck, Observation of a Dissipative Phase Transition in a One-Dimensional Circuit QED Lattice, *Phys. Rev. X* **7**, 011016 (2017).

- [11] M. Malekakhlagh, A. Petrescu, and H. E. Türeci, Lifetime renormalization of weakly anharmonic superconducting qubits. I. Role of number nonconserving terms, *Phys. Rev. B* **101**, 134509 (2020).
- [12] A. Petrescu, M. Malekakhlagh, and H. E. Türeci, Lifetime renormalization of driven weakly anharmonic superconducting qubits. II. The readout problem, *Phys. Rev. B* **101**, 134510 (2020).
- [13] E. M. Purcell, H. C. Torrey, and R. V. Pound, Resonance absorption by nuclear magnetic moments in a solid, *Phys. Rev.* **69**, 37 (1946).
- [14] D. Sank, Z. Chen, M. Khezri, J. Kelly, R. Barends, B. Campbell, Y. Chen, B. Chiaro, A. Dunsworth, A. Fowler, E. Jeffrey, E. Lucero, A. Megrant, J. Mutus, M. Neeley, C. Neill, P. J. J. O'Malley, C. Quintana, P. Roushan, A. Vainsencher *et al.*, Measurement-Induced State Transitions in a Superconducting Qubit: Beyond the Rotating Wave Approximation Daniel, *Phys. Rev. Lett.* **117**, 190503 (2016).
- [15] Z. K. Mineev, S. O. Mundhada, S. Shankar, P. Reinhold, R. Gutiérrez-Jáuregui, R. J. Schoelkopf, M. Mirrahimi, H. J. Carmichael, and M. H. Devoret, To catch and reverse a quantum jump mid-flight, *Nature (London)* **570**, 200 (2019).
- [16] D. H. Slichter, C. Müller, R. Vijay, S. J. Weber, A. Blais, and I. Siddiqi, Quantum Zeno effect in the strong measurement regime of circuit quantum electrodynamics, *New J. Phys.* **18**, 053031 (2016).
- [17] S. E. Nigg, H. Paik, B. Vlastakis, G. Kirchmair, S. Shankar, L. Frunzio, M. H. Devoret, R. J. Schoelkopf, and S. M. Girvin, Black-Box Superconducting Circuit Quantization, *Phys. Rev. Lett.* **108**, 240502 (2012).
- [18] A. C. Y. Li, F. Petruccione, and J. Koch, Perturbative approach to markovian open quantum systems, *Sci. Rep.* **4**, 4887 (2014).
- [19] A. C. Y. Li, F. Petruccione, and J. Koch, Resummation for Nonequilibrium Perturbation Theory and Application to Open Quantum Lattices, *Phys. Rev. X* **6**, 021037 (2016).
- [20] J. Koch, T. M. Yu, J. Gambetta, A. A. Houck, D. I. Schuster, J. Majer, A. Blais, M. H. Devoret, S. M. Girvin, and R. J. Schoelkopf, Charge-insensitive qubit design derived from the cooper pair box, *Phys. Rev. A* **76**, 042319 (2007).
- [21] In the regime of interest, there are many localized-in-phase energy levels associated with the transmon, and the instability physics studied in Ref. [39] plays no role.
- [22] Our focus here is on Purcell decay: understanding how cavity dissipation gives rise to qubit relaxation. We note that high-frequency qubit dephasing noise can also lead to photon-number dependent qubit population decay. This dressed-dephasing mechanism [40,41] is expected to be suppressed in systems where dephasing is weak and primarily due to low-frequency noise.
- [23] Note that Refs. [11,12] use an alternate approach that also avoids making unjustified secular approximations. Their approach captures some but not all aspects of our correlated-dissipation master equation (whose form follows from an exact derivation).
- [24] S. Chaturvedi and V. Srinivasan, Class of exactly solvable master equations describing coupled nonlinear oscillators, *Phys. Rev. A* **43**, 4054 (1991).
- [25] M. I. Dykman and M. A. Krivoglaz, *Soviet Physics Reviews* (Harwood Academic, Reading, UK, 2011).
- [26] D. Honda, H. Nakazato, and M. Yoshida, Spectral resolution of the liouvillian of the lindblad master equation for a harmonic oscillator, *J. Math. Phys.* **51**, 072107 (2010).
- [27] O. Scarlatella, A. A. Clerk, and M. Schiro, Spectral functions and negative density of states of a driven-dissipative nonlinear quantum resonator, *New J. Phys.* **21**, 043040 (2019).
- [28] J. R. Johansson, P. D. Nation, and F. Nori, Qutip: An open-source python framework for the dynamics of open quantum systems, *Comput. Phys. Commun.* **183**, 1760 (2012).
- [29] J. R. Johansson, P. D. Nation, and F. Nori, Qutip 2: A Python framework for the dynamics of open quantum systems, *Comput. Phys. Commun.* **184**, 1234 (2013).
- [30] M.-A. Lemonde and A. A. Clerk, Real photons from vacuum fluctuations in optomechanics: The role of polariton interactions, *Phys. Rev. A* **91**, 033836 (2015).
- [31] A. A. Clerk, M. H. Devoret, S. M. Girvin, F. Marquardt, and R. J. Schoelkopf, Introduction to quantum noise, measurement, and amplification, *Rev. Mod. Phys.* **82**, 1155 (2010).
- [32] A. Kamenev, *Field Theory of Non-Equilibrium Systems* (Cambridge University Press, Cambridge, 2011).
- [33] L. M. Sieberer, M. Buchhold, and S. Diehl, Keldysh field theory for driven open quantum systems, *Rep. Prog. Phys.* **79**, 096001 (2016).
- [34] C. Gardiner and P. Zoller, *Quantum Noise: A Handbook of Markovian and non-Markovian Quantum Stochastic Methods with Applications to Quantum Optics* (Springer Science & Business Media, New York, 2004).
- [35] J. J. Sakurai, *Modern Quantum Mechanics* (Addison Wesley, Reading, MA, 1993).
- [36] T. Prosen and T. H. Seligman, Quantization over boson operator spaces, *J. Phys. A: Math. Theor.* **43**, 392004 (2010).
- [37] T. Prosen, Third quantization: a general method to solve master equations for quadratic open fermi systems, *New J. Phys.* **10**, 043026 (2008).
- [38] Y. Zhang, J. C. Curtis, C. S. Wang, R. J. Schoelkopf, and S. M. Girvin, Drive-induced nonlinearities of cavity modes coupled to a transmon ancilla [arXiv:2106.09112](https://arxiv.org/abs/2106.09112).
- [39] L. Verney, R. Lescanne, M. H. Devoret, Z. Leghtas, and M. Mirrahimi, Structural Instability of Driven Josephson Circuits Prevented by an Inductive Shunt, *Phys. Rev. Applied* **11**, 024003 (2019).
- [40] M. Boissonneault, J. M. Gambetta, and A. Blais, Nonlinear dispersive regime of cavity qed: The dressed dephasing model, *Phys. Rev. A* **77**, 060305(R) (2008).
- [41] D. H. Slichter, R. Vijay, S. J. Weber, S. Boutin, M. Boissonneault, J. M. Gambetta, A. Blais, and I. Siddiqi, Measurement-Induced Qubit State Mixing in Circuit QED from Up-Converted Dephasing Noise, *Phys. Rev. Lett.* **109**, 153601 (2012).